ESL-TR-92-65

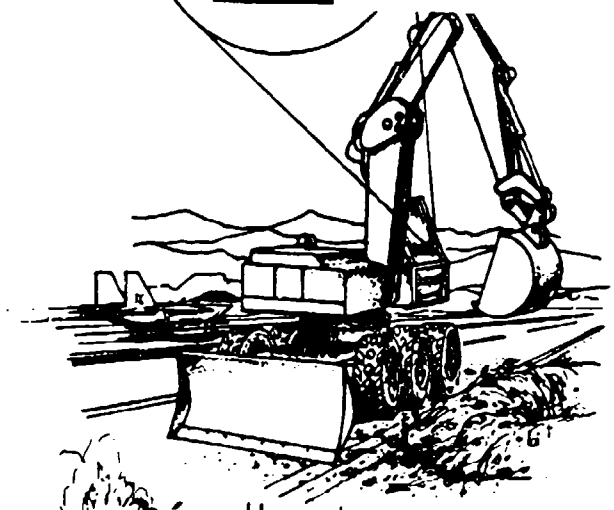

EQUIPMENT SHOCK TOLERANCE

D.H. MERKLE, M.A. ROCHEFORT,
C.Y. TUAN

APPLIED RESEARCH ASSOCIATES
2101 SAN MATEO BLVD
SUITE A220
ALBUQUERQUE NM 87110

APRIL 1993

FINAL REPORT

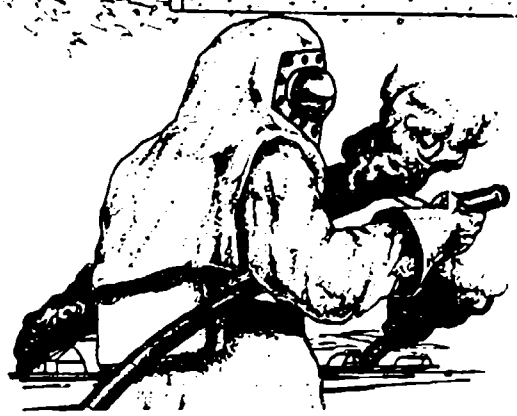

FEBRUARY 1992 - NOVEMBER 1992

**APPROVED FOR PUBLIC RELEASE:
DISTRIBUTION UNLIMITED**

ENGINEERING RESEARCH DIVISION
Air Force Civil Engineering Support Agency
Civil Engineering Laboratory
Tyndall Air Force Base, Florida 32403

NOTICE

PLEASE DO NOT REQUEST COPIES OF THIS REPORT FROM HQ AFCESA/RA (AIR FORCE CIVIL ENGINEERING SUPPORT AGENCY). ADDITIONAL COPIES MAY BE PURCHASED FROM:

NATIONAL TECHNICAL INFORMATION SERVICE
5285 PORT ROYAL ROAD
SPRINGFIELD, VIRGINIA 22161

FEDERAL GOVERNMENT AGENCIES AND THEIR CONTRACTORS REGISTERED WITH DEFENSE TECHNICAL INFORMATION CENTER SHOULD DIRECT REQUESTS FOR COPIES OF THIS REPORT TO:

DEFENSE TECHNICAL INFORMATION CENTER
CAMERON STATION
ALEXANDRIA, VIRGINIA 22314

REPORT DOCUMENTATION PAGE

Form Approved
OMB No. 0704-0188

1. AGENCY USE ONLY (Leave blank)	2. REPORT DATE	3. REPORT TYPE AND DATES COVERED
	April 1993	Final report; From 92 02 To 92 11

4. TITLE AND SUBTITLE

Equipment Shock Tolerance

5. FUNDING NUMBERS

F08635-88-C-0067

6. AUTHOR(S)

Merkle, D.H.; Rochefort, M.A.; Tuan, C.Y.

7. PERFORMING ORGANIZATION NAME(S) AND ADDRESS(ES)

Applied Research Associates, Inc.
2101 San Mateo Blvd. NE, Suite A220
Albuquerque, NM 87110

8. PERFORMING ORGANIZATION REPORT NUMBER

9. SPONSORING/MONITORING AGENCY NAME(S) AND ADDRESS(ES)

U. S. Air Force Civil Engineering Support Agency
Tyndall Air Force Base, FL 32403-6001

10. SPONSORING/MONITORING AGENCY REPORT NUMBER

ESL-TR-92-65

11. SUPPLEMENTARY NOTES

12a. DISTRIBUTION/AVAILABILITY STATEMENT

This report has been reviewed by the Public Affairs Office and is releasable to the National Technical Information Service (NTIS). At NTIS, it will be available to general public, including foreign nations.

12b. DISTRIBUTION CODE

13. ABSTRACT *(Maximum 200 words)*

The objective of this research effort was to assess the accuracy of using the shock response spectrum (SRS) for defining equipment shock tolerance. The focus of the research was on mission-critical equipment installed in airbase hardened structures, designed to survive the airblast and ground shock effects of a close-in detonation by a modern, nonnuclear weapon. The motivation was the prospect of improving the shock tolerance of such equipment, by first improving equipment shock tolerance characterization, thereby improving knowledge of the factors controlling equipment shock tolerance. Two simple mathematical equipment models were developed to quantify some of the errors introduced by assessing the shock tolerance of equipment via the classic, linear, SDoF shock response spectrum. The effects of waveform dependency of equipment shock response; multi-degree-of-freedom (MDoF) vs. SDoF equipment response; multidirectional loading on equipment response; and geometric nonlinearity on equipment response were investigated. This study has proven the inadequacy of the linear, SDoF shock response spectrum for characterizing the shock tolerance of equipment. Complex, nonlinear mechanical equipment subjected to multi-directional support motion cannot be adequately represented by an SDoF SRS.

14. SUBJECT TERMS	15. NUMBER OF PAGES
Equipment fragility, Ground shock, Mathematical models, Modal analysis, Shock response spectrum, Structural dynamics	63
	16. PRICE CODE

17. SECURITY CLASSIFICATION OF REPORT	18. SECURITY CLASSIFICATION OF THIS PAGE	19. SECURITY CLASSIFICATION OF ABSTRACT	20. LIMITATION OF ABSTRACT
UNCLASSIFIED	UNCLASSIFIED	UNCLASSIFIED	UL

(The reverse of this page is blank.)

EXECUTIVE SUMMARY

A. OBJECTIVE

The objective of this research effort was to assess the accuracy of using the shock response spectrum (SRS) for defining equipment shock tolerance. The focus of the research was on mission-critical equipment installed in airbase hardened structures, designed to survive the airblast and ground shock effects of a close-in detonation by a modern, nonnuclear weapon. The motivation was the prospect of improving the shock tolerance of such equipment, by first improving equipment shock tolerance characterization, thereby improving knowledge of the factors controlling equipment shock tolerance.

B. BACKGROUND

A shock response spectrum is a plot of the maximum response amplitude of a damped single-degree-of-freedom (SDoF) oscillator subjected to support excitation, as a function of the natural frequency and damping value of the oscillator. An SRS is a convenient means of illustrating the peak response of a collection of SDoF systems to a particular shock excitation. Due to its simplicity, the SRS has become widely employed as a means of describing the shock response of structures and equipment.

Since in-structure motions are typically described using shock response spectra (actually tripartite shock response spectra), it was only natural to attempt to quantify equipment failure in terms of shock spectra. The advantage of expressing equipment failure with the same representation used to quantify the in-structure shock environment is obvious. Expressing equipment fragility in terms of shock response spectra greatly simplifies the design of equipment shock isolation.

The approach employed to determine equipment fragility is to subject an item of equipment to a base motion of a certain intensity, frequency, etc. If the equipment does not fail, the intensity of the base motion is increased until failure occurs. The shock response spectrum of the base motion which just causes the equipment to fail is called the shock tolerance spectrum, or the fragility spectrum of the equipment, even though the test SRS is input waveform-dependent.

By comparing the fragility spectrum of an item of equipment to the in-structure SRS at the proposed equipment location, shock isolation requirements are easily assessed. If the equipment fragility spectrum exceeds the in-structure SRS at all frequencies, no shock isolation is required.

If the in-structure SRS exceeds the equipment fragility spectrum at any frequency, shock isolation is required.

This approach to shock isolation assessment is oversimplified, and ignores several sources of error. The most important source of error is the fact that an SRS does not correspond to a unique input time-history. An infinite number of different base motions can generate a given SRS. These different base motions could vary greatly in duration, frequency content, and amplitude. The main assumption behind the SRS approach to equipment fragility is that equipment failure is independent of the input waveform. It is assumed that the frequency content of the support motion does not play a role in equipment failure. All input base motions are assumed to result in the same failure mode. The possibility of a single item of equipment possessing multiple failure modes is not considered. In reality, equipment fragility spectra are probably only valid for frequencies close to the frequency at which the item of equipment was actually tested. Extrapolating equipment fragility based on nuclear testing to the conventional weapon environment is now done routinely. The validity of this extrapolation has never been verified.

C. SCOPE

This report quantifies some of the errors introduced by assessing the shock tolerance of equipment via the classic, linear, SDoF shock response spectrum. Two simple mathematical equipment models were developed for the investigation: (1) a spring pendulum, which possesses two degrees of freedom and geometric nonlinearity, and (2) a clamped beam carrying a tip mass having both translational and rotary inertia, which possesses an infinite number of linear, orthogonal modes. These models were used to investigate the effect of factors such as: waveform dependency of equipment shock response; multi-degree-of-freedom (MDoF) vs. SDoF equipment response; the effect of multidirectional loading on equipment response; and the effect of geometric nonlinearity on equipment response.

D. CONCLUSIONS

This study uncovered and quantified several shortcomings of the SRS approach to characterizing equipment shock tolerance:

- It was proven that SRS-based fragility spectra are not unique. Even for an item of equipment which can be modeled by a simple SDoF undamped oscillator, each different base excitation produces a different fragility spectrum.
- The spring pendulum model was used to illustrate the response of a geometrically nonlinear item of equipment to two-dimensional base motion. It was shown that extremely erratic

behavior is possible if the frequency of the base motion approaches one of the natural frequencies of the equipment model. The maximum response can be several times greater than that of a simple SDoF oscillator.

- The cantilever beam model was used to show that the maximum repsonse of an MDoF system will always exceed the response of a simple oscillator.

In conclusion, this study has proven the inadequacy of the linear, SDoF shock response spectrum for characterizing the shock tolerance of equipment. Complex, nonlinear mechanical equipment subjected to multi-directional support motion cannot be adequately represented by an SDoF SRS.

E. RECOMMENDATIONS

Based on the results of this study, a more rigorous approach for assessing equipment shock tolerance is required. The following points should be kept in mind while developing this new procedure:

- When an item of equipment is tested to determine its shock tolerance, the test input waveform must be representative of the anticipated threat input waveform. Multi-directional support motion must be reproduced. Equipment tests should excite the same response modes, and produce the same failure modes, as the actual in-service base motion.
- Analytical equipment models must be detailed enough to reproduce the salient features of the actual equipment response. The model need not encompass the entire item of equipment, but it must adequately represent the critical components. The input motion to the model must mimic the in-service motion.

(The reverse of this page is blank.)

PREFACE

This report was prepared by Applied Research Associates, Inc., P.O. Box 40128, Tyndall Air Force Base, FL 32403, under Scientific and Engineering Technical Assistance (SETA) contract F08635-88-C-0067 with the Air Force Civil Engineering Support Agency, Engineering Research Division (AFCESA/RAC), Tyndall Air Force Base, FL 32403.

The Air Force Project Monitors for this subtask were: Dr. Michael G. Katona, Mr. William S. Strickland, and Mr. Edgar F. Alexander.

This report has been reviewed by the Public Affairs Office and is releasable to the National Technical Information Service (NTIS). At NTIS, it will be available to the general public, including foreign nations.

This technical report has been reviewed and is approved for publication.

William S. Strickland
WILLIAM S. STRICKLAND
Chief, Airbase Survivability Section

Felix T. Uhlik, III
FELIX T. UHLIK, III, Lt Col, USAF
Chief, Engineering Research Branch

(The reverse of this page is blank)

TABLE OF CONTENTS

LIST OF FIGURES

LIST OF FIGURES
(Continued)

SECTION I

INTRODUCTION

A. OBJECTIVE

The objective of this research effort was to assess the accuracy of using the shock response spectrum (SRS) for defining equipment shock tolerance. The focus of the research was on mission-critical equipment installed in airbase hardened structures, designed to survive the airblast and ground shock effects of a close-in detonation by a modern, nonnuclear weapon. The motivation was the prospect of improving the shock tolerance of such equipment, by first improving equipment shock tolerance characterization, thereby improving knowledge of the factors controlling equipment shock tolerance.

B. BACKGROUND

A shock response spectrum is a plot of the maximum response amplitude of a damped single-degree-of-freedom (SDoF) oscillator subjected to support excitation, as a function of the natural frequency and damping value of the oscillator. For the SDoF oscillator shown in Figure 1, the response is controlled by three parameters: the mass, m; spring stiffness, k; and damping coefficient, c. If the base motion (i.e., shock excitation) is described by a displacement time-history, $y(t)$; and the resulting displacement of the mass is given by $x(t)$; the relative displacement between the mass and the base may be calculated as, $u(t) = x(t) - y(t)$. The peak SDoF system responses of most interest in shock analysis are: the maximum absolute value of relative displacement between the mass and base (spectral displacement, S_d); the maximum absolute value of relative velocity between the mass and base (approximated by the spectral velocity, S_v); and the maximum absolute value of mass acceleration (approximated by the spectral acceleration, S_a). The three spectral quantities are related by the following defining equation

$$\frac{1}{\omega_n} S_a = S_v = \omega_n S_d \tag{1}$$

where

$$\omega_n = \sqrt{\frac{k}{m}} \qquad \text{(rad/sec)} \tag{2}$$

is the natural circular frequency of the SDoF system. This relationship allows spectral

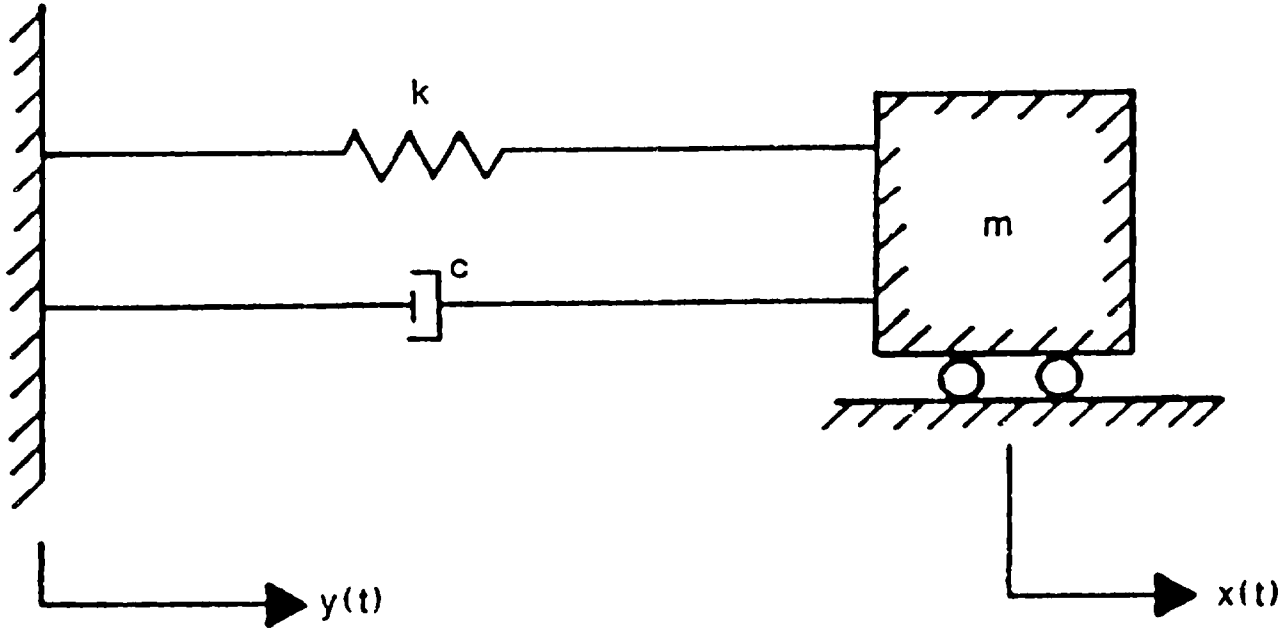

$$u = x - y$$

Figure 1. Single-Degree-of-Freedom Oscillator Subjected to Base Motion.

displacement, velocity, and acceleration to be plotted on a single graph, as a function of system natural circular frequency, ω_n; or system natural frequency, f_n; where

$$f_n = \frac{\omega_n}{2\pi} \qquad \text{(Hz)} \qquad (3)$$

Such a plot is referred to as a tripartite shock response spectrum. Typical tripartite shock response spectra are shown in Figure 2. It is common for a tripartite shock response spectrum to be referred to simply as a shock response spectrum.

A SRS is a convenient means of illustrating the peak response of a collection of SDoF systems to a particular shock excitation. Due to its simplicity, the SRS has become widely employed as a means of describing the shock response of structures and equipment. Years of earthquake research have shown that all earthquake shock response spectra display similar characteristics. In fact, it has been shown that approximate upper bound response spectra may be constructed, based only on the peak displacement, velocity and acceleration of the oscillator base. For SDoF systems damped at between 5 and 10 percent of critical damping, an approximate SRS can be constructed by simply multiplying the peak displacement, velocity and acceleration of the base by factors of 1.0, 1.5, and 2.0, respectively. Approximate shock response spectra generated by this approach are assumed to represent the upper bound of the actual shock response spectra, and are further considered to be independent of the precise form of the input motion.

A technique similar to that described above for bounding earthquake shock response spectra has been adopted by conventional weapon effects analysts. Kiger, et. al. (1984), have shown that in-structure shock response spectra can be bounded by multiplying the peak in-structure displacement, velocity, and acceleration by factors of 1.2, 1.5, and 2.0, respectively. Shock response spectra generated by this technique are assumed to give an upper bound on the response of a damped (5 to 10 percent of critical) oscillator located near the center of a buried facility.

Since in-structure motions are typically described using shock response spectra (actually tripartite shock response spectra), it was only natural to attempt to quantify equipment failure in terms of shock spectra. The advantage of expressing equipment failure with the same representation used to quantify the in-structure shock environment is obvious. Expressing equipment fragility in terms of shock response spectra greatly simplifies the design of equipment shock isolation.

The approach employed to determine equipment fragility is to subject an item of equipment to a base motion of a certain intensity, frequency, etc. If the equipment does not fail, the intensity of the base motion is increased until failure occurs. The shock response spectrum of the base motion which just causes the equipment to fail is called the shock tolerance spectrum, or the fragility spectrum of the equipment, even though the test SRS is input waveform-dependent.

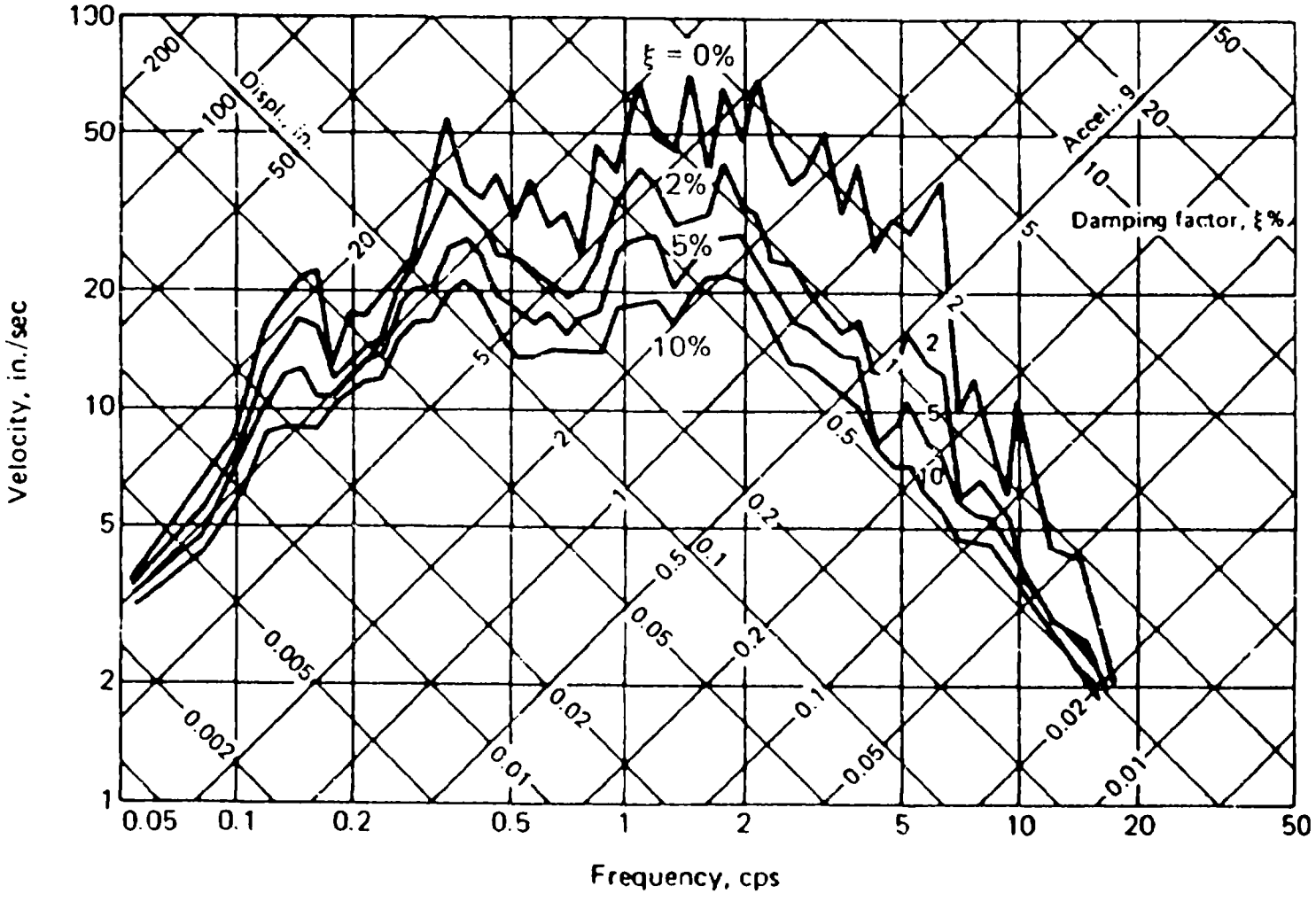

Figure 2. Tripartite Response Spectra for Damping Ratios of 0, 2, 5 and 10 Percent of Critical (Paz,1985).

By comparing the fragility spectrum of an item of equipment to the in-structure SRS at the proposed equipment location, shock isolation requirements are easily assessed. If the equipment fragility spectrum exceeds the in-structure SRS at all frequencies, no shock isolation is required. If the in-structure SRS exceeds the equipment fragility spectrum at any frequency, shock isolation is required.

This approach to shock isolation assessment is oversimplified, and ignores several sources of error. The most important source of error is the fact that an SRS does not correspond to a unique input time-history. An infinite number of different base motions can generate a given SRS. These different base motions could vary greatly in duration, frequency content, and amplitude. The main assumption behind the SRS approach to equipment fragility is that equipment failure is independent of the input waveform. In reality, equipment fragility spectra are probably only valid for waveforms resembling the one under which the item of equipment was actually tested. Extrapolating equipment fragility based on nuclear testing to the conventional weapon environment is now done routinely. The validity of this extrapolation has never been verified.

C. SCOPE

This report quantifies some of the errors introduced by assessing the shock tolerance of equipment via the classic, linear, SDoF shock response spectrum. Two simple mathematical equipment models were developed for the investigation: (1) a spring pendulum, which possesses two degrees of freedom and geometric nonlinearity, and (2) a clamped beam carrying a tip mass having both translational and rotary inertia, which possesses an infinite number of linear, orthogonal modes. These models were used to investigate the effect of factors such as: waveform dependency of equipment shock response; multi-degree-of-freedom (MDoF) vs. SDoF equipment response; the effect of multidirectional loading on equipment response, and the effect of geometric nonlinearity on equipment response.

SECTION II

LITERATURE REVIEW

A. INTRODUCTION

The literature on equipment shock tolerance is extensive. It includes literature on methods of analyzing the transient response of mechanical systems to shock input, the origin of and assumptions underlying the shock response spectrum, observed equipment damage due to shock, equipment shock testing methods, and equipment shock test data analysis and interpretation. Since the purpose of this effort is to examine the accuracy of the shock response spectrum in predicting the shock tolerance of a representative equipment subsystem, an examination of the history of the shock response spectrum was in order. This inquiry led to a cursory but fascinating review of the theory of the transient response of linear systems, as developed by well-known mathematicians and engineers including Cauchy, Heaviside, Steinmetz, Carson, Bush, Biot, Housner, and Gardner and Barnes.

Heaviside has been credited with the development of much of modern operational system theory, and Bush's book reinforces that notion. However, as Bush and colleagues, Gardner and Barnes, studied the subject further, it became clear that Heaviside had ignored more fundamental methods developed earlier by Cauchy and other mathematicians. Steinmetz, often credited with introducing complex numbers into AC circuit analysis, gets no credit from Bush or Gardner and Barnes. Biot's Ph.D. thesis, written at Cal Tech in 1932 under Von Karman, applied complex variable methods to transient, linear structural dynamics, but the shock response spectrum concept is not clearly evident there. It is clearly evident in Housner's 1941 Cal Tech Ph.D. thesis. It was Jacobsen, Crede, and particularly Newmark who popularized the shock response spectrum concept in protective constuction shock isolation analysis.

B. EQUIPMENT FRAGILITY BASED ON THE SRS METHOD

Current design guidelines for isolating equipment from the effects of conventional weapon-induced structural motions are based on SAFEGUARD test data. The SAFEGUARD Hardness Assurance Program was conducted to investigate the reliability of equipment installed in hardened Ballistic Missile Defense (BMD) facilities. In SAFEGUARD, some 300 items of off-the-shelf commercial equipment, assigned to 32 generic equipment groups, were tested to qualify 30,000 critical items located in SAFEGUARD installations. Both electical and mechanical components were subjected to shake-table testing. The base motion consisted of a sine sweep pulse of 5

second duration, selected to fit a prescribed acceleration spectrum. The prescribed acceleration spectrum was based on calculations of the shock environment within the SAFEGUARD BMD facility.

Initially, fragility testing was conducted on selected equipment items, but most of the testing was limited to proof-type qualification tests, i.e. tests performed at shock input levels at or below design levels, to qualify the equipment for operational service. Most SAFEGUARD data is given in terms of the base motion SRS that the equipment survived in proof-type qualification tests. In most cases there is no indication of how close the SRS is to the failure threshold of the equipment. In addition, much of the data does not encompass the sensitive frequencies for the items of equipment.

Despite the obvious limitations of the SAFEGUARD data, all land-based equipment shock isolation designs are currently based on this information. The SAFEGUARD procedure is recommended by both the Army's Fundamentals of Protective Design for Conventional Weapons and the Air Force's Protective Construction Design Manual, because a better procedure is not yet available.

SECTION III

EQUIPMENT SHOCK RESPONSE

A. INTRODUCTION

The previous sections have raised several questions regarding the validity of defining equipment shock tolerance via the tripartite SRS. The objective of this section is to quantify the magnitude of the errors introduced by the SRS approach . Two analytical models were developed for this purpose: (1) a spring pendulum, and (2) a clamped beam carrying a tip mass.

B. FRAGILITY SPECTRA FROM AN IDEAL EXPERIMENT

The greatest error associated with the SRS approach to equipment shock tolerance characterization lies in the assumption that the shock tolerance of the equipment is independent of the precise input waveform. To examine the validity of this assumption, the authors designed a perfect *analytical experiment* using an ideal item of equipment with known fragility. It was assumed that the item of equipment is perfectly modeled by an SDoF undamped oscillator with a natural frequency of 25 Hz. This simple item of equipment was assumed to fail when the relative displacement between the mass and the support reached a value of 0.25 inches.

Fragility testing of this simple SDoF equipment item was conducted analytically. The support excitation was a half-cycle sine velocity pulse of the form

$$\dot{y}(t) = V_{max} \sin\left(\frac{\pi}{t_d}\right)t \qquad \text{for} \qquad 0 \le t \le t_d \tag{4}$$

and

$$\dot{y}(t) = 0 \qquad \text{otherwise} \tag{5}$$

where V_{max} is the amplitude of the pulse, and t_d is the duration.

The first fragility test was conducted for a half-cycle sine velocity pulse with a duration of 1 second. The amplitude of the support motion was increased until the maximum relative displacement reached a value of 0.25 inches. Equipment failure occured when the amplitude of the sine pulse reached a value of 982 in/sec.

A second fragility test was performed with a pulse duration of 0.01 seconds. The pulse amplitude producing failure was 42 in/sec.

Thus, we now have two half-cycle sine velocity pulses which will just precipitate failure in the ideal SDoF 25 Hz item of equipment. The maximum relative displacement spectra for these two sine pulses are shown in Figure 3. Notice that the two spectra coincide at only a single point (Frequency = 25 Hz).

The tripartite shock response spectra for the two half-cycle sine base excitations are shown in Figure 4. Again, notice that the spectra coincide at only one point (the point at which they were forced to agree). Which of these two spectra is the correct fragility spectrum for the item of equipment? Neither one! There are an infinite number of possible fragility spectra for this simple item of equipment. The only similarity between these spectra is the fact that they all intersect at a frequency of 25 Hz and an amplitude of 0.25 in.

This analytical experiment clearly illustrates the inadequacy of SRS-based fragility characterization.

C. EFFECT OF TWO-DIMENSIONAL BASE MOTION ON EQUIPMENT RESPONSE

An item of equipment located in a hardened shelter will be subjected to three-dimensional support motion. In all likelihood, the equipment item possesses multiple degrees of freedom, and exhibits nonlinear response to shock input. The obvious question is -- what is the error introduced by modeling a nonlinear MDoF item of equipment subject to three-dimensional support motion, with a linear SDoF oscillator?

To begin a quantitative investigation of this question, an equipment model capable of responding to multi-directional support motion was required. A simple two-dimensional spring pendulum equipment model was developed for the investigation (see Figure 5). This simple model possesses two degrees of freedom and geometric nonlinearity. The model is capable of responding to horizontal and vertical support motion, individually or in combination. The complete mathematical development of the spring pendulum model is presented in Appendix A. The computational algorithm described in Appendix A was coded into a FORTRAN computer program named SPEND. A listing of SPEND is included as Appendix B.

The spring pendulum equipment model exhibits characteristics of both a spring-mass oscillator and a simple pendulum. Thus, it possesses two characteristic natural frequencies of interest; the natural frequency of a simple pendulum, given by

$$f_{pendulum} = \frac{1}{2\pi}\sqrt{\frac{g}{l}} \qquad \text{(Hz)} \qquad (6)$$

where g is the acceleration due to gravity, and l is the length of the pendulum; and the natural frequency of a simple spring-mass oscillator, given by

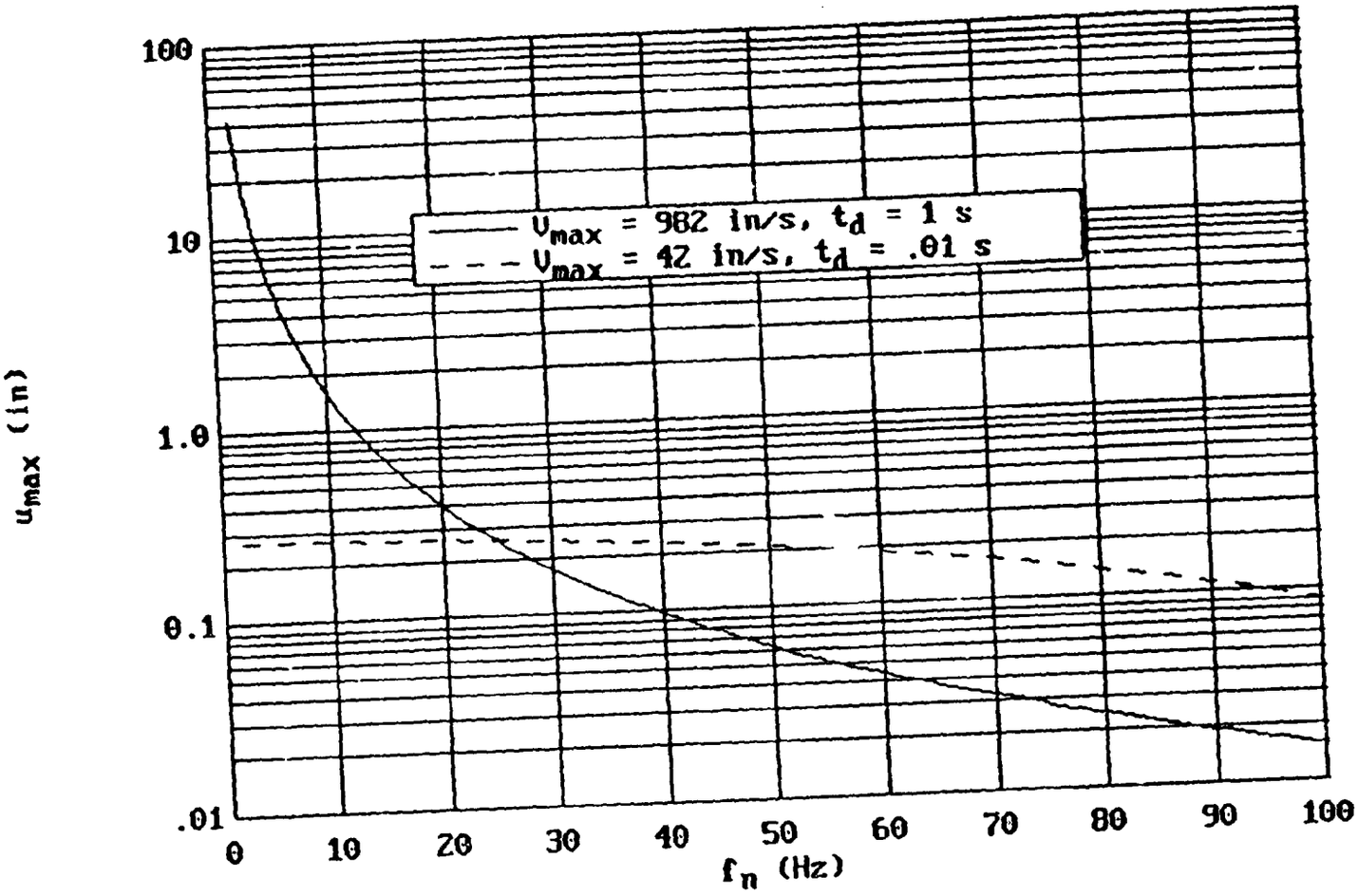

Figure 3. Maximum Relative Displacement vs. Frequency for Half-Cycle Sine Velocity Pulses (Fragility: u_{max} = 0.25 inches @ f_n = 25 Hz).

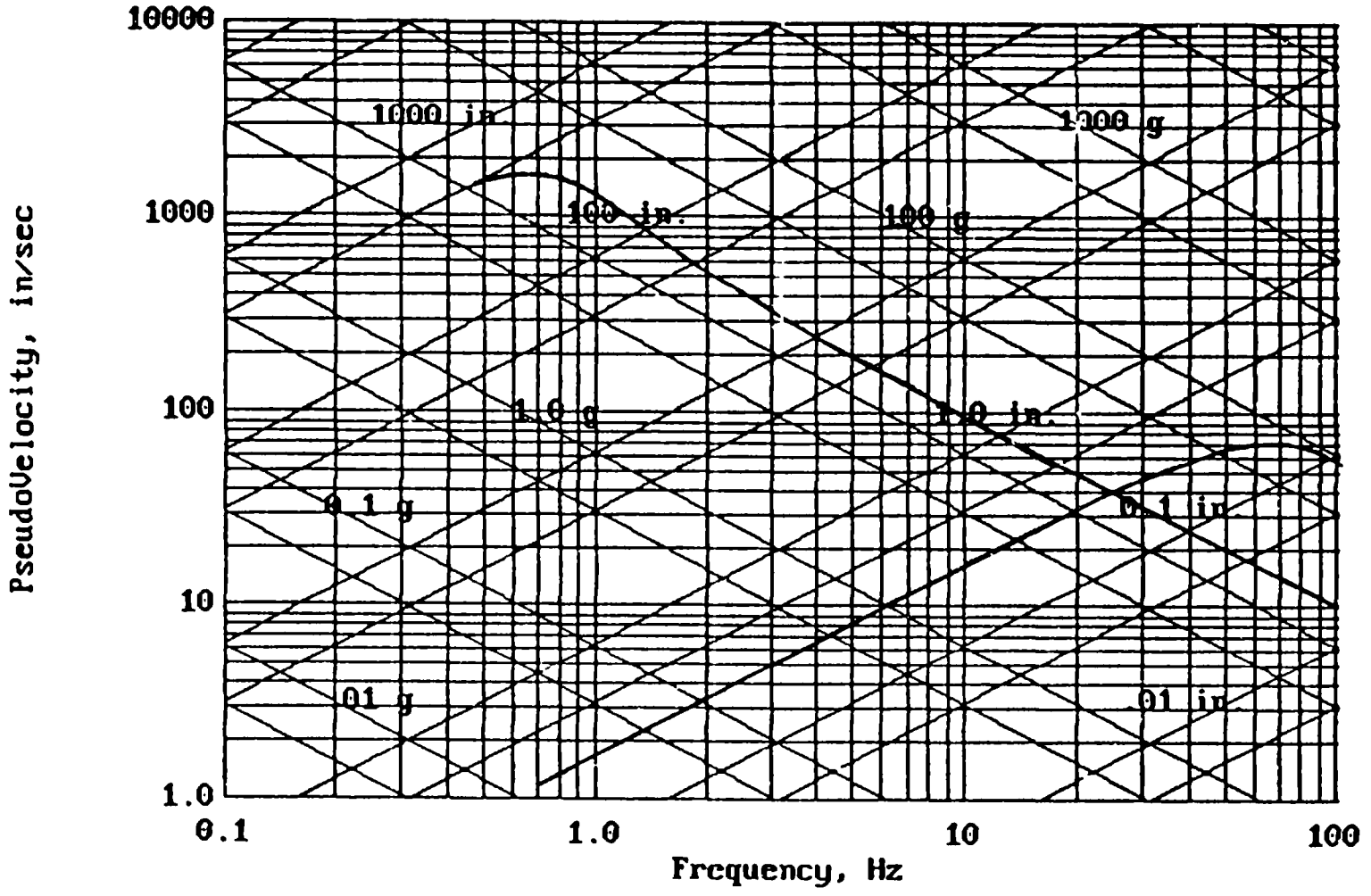

Figure 4. Shock Response Spectra for Half-Cycle Sine Velocity Pulses.

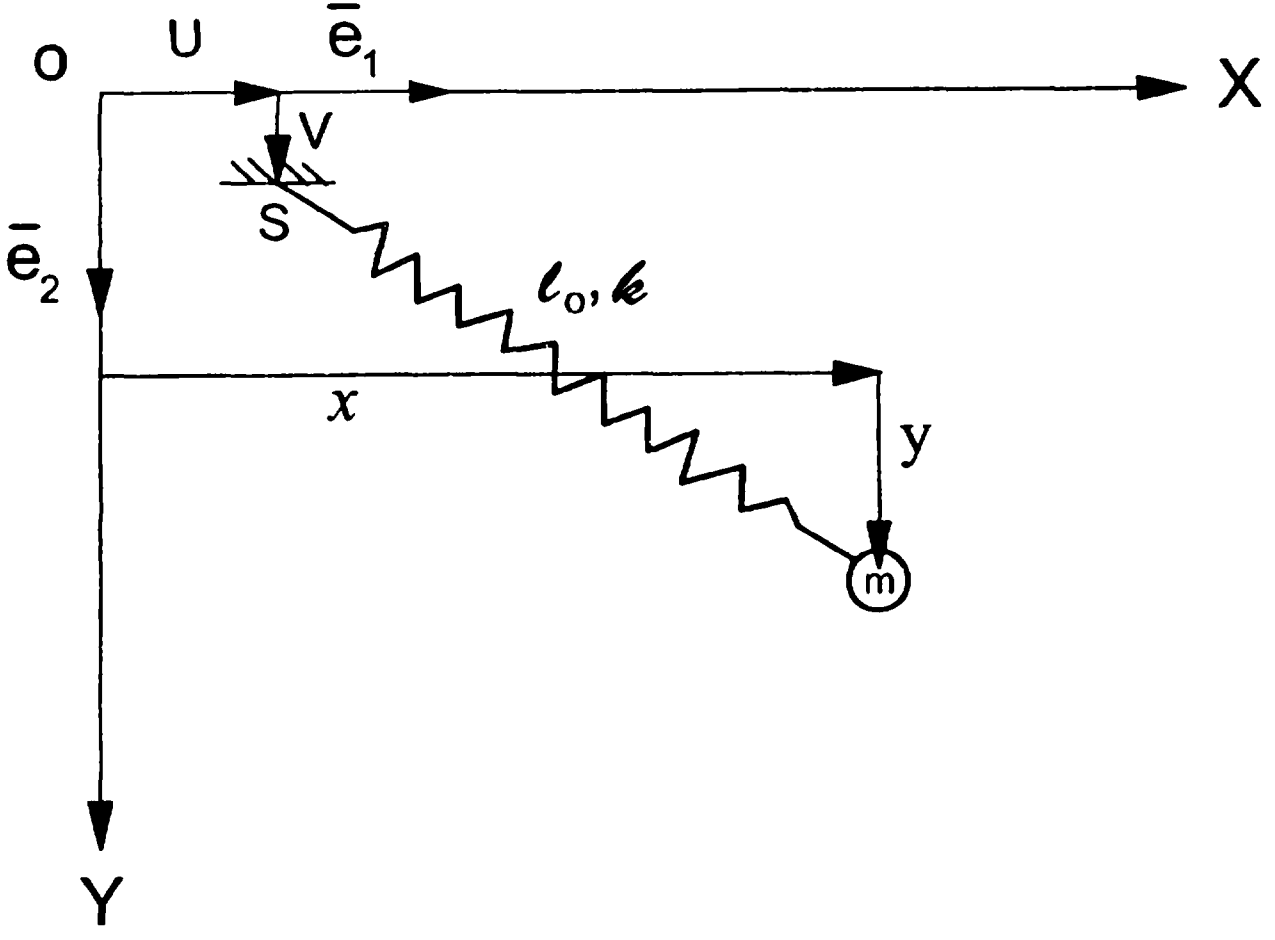

Figure 5. Spring Pendulum Equipment Model.

$$f_{spring-mass} = \frac{1}{2\pi}\sqrt{\frac{k}{m}} \qquad \text{(Hz)} \qquad (7)$$

where k is the spring stiffness, and m is the oscillator mass.

A parameter study was performed to investigate the response of the spring pendulum subjected to simultaneous horizontal and vertical support motion. As a baseline for comparison, the response to the superimposed motion was compared to the response due to vertical base motion only. The support motion for all cases was a half-cycle sine velocity pulse of the form described in Equations (4) and (5). All support motions had an amplitude of 20 in/sec. Pulse durations varied from 0.05 to 0.5 seconds.

The first set of calculations were performed using velocity pulses with a duration of 0.05 seconds. The results are given in Figure 6. The solid line in Figure 6 represents the response of the spring pendulum subjected to vertical support motion only. This response mode corresponds to a simple 1-D spring-mass oscillator. The three remaining curves represent the response of the spring pendulum when subjected to both horizontal and vertical support motion simultaneously. Notice that biaxial support motion always results in a spring force greater than that caused by vertical support motion only. The amplification of the spring force increases as the pendulum frequency approaches the frequency of the support motion.

Figure 7 presents the results of calculation set number 2. For this run, the pulse durations were all 0.1 second.

The results of the third calculation set are given in Figure 8. The support motions for these calculations had a duration of 0.25 seconds. This corresponds to a frequency of approximately 4 Hz. Notice the marked increase in the spring pendulum response for the pendulum frequency of 3 Hz.

Results of the last calculation set are given in Figure 9. The duration of the support motion for this set was 0.5 seconds (frequency ~ 2 Hz). Notice the response of the spring pendulum for the pendulum frequency of 2 Hz. When the frequency of the support motion and the pendulum frequency of the spring pendulum model coincide, the response of the model becomes erratic.

Figure 9 clearly illustrates what is possible when a nonlinear equipment item with certain fundamental frequencies is subjected to biaxial support motion. The maximum response of such an equipment item could be many times greater than the response calculated using a simple oscillator.

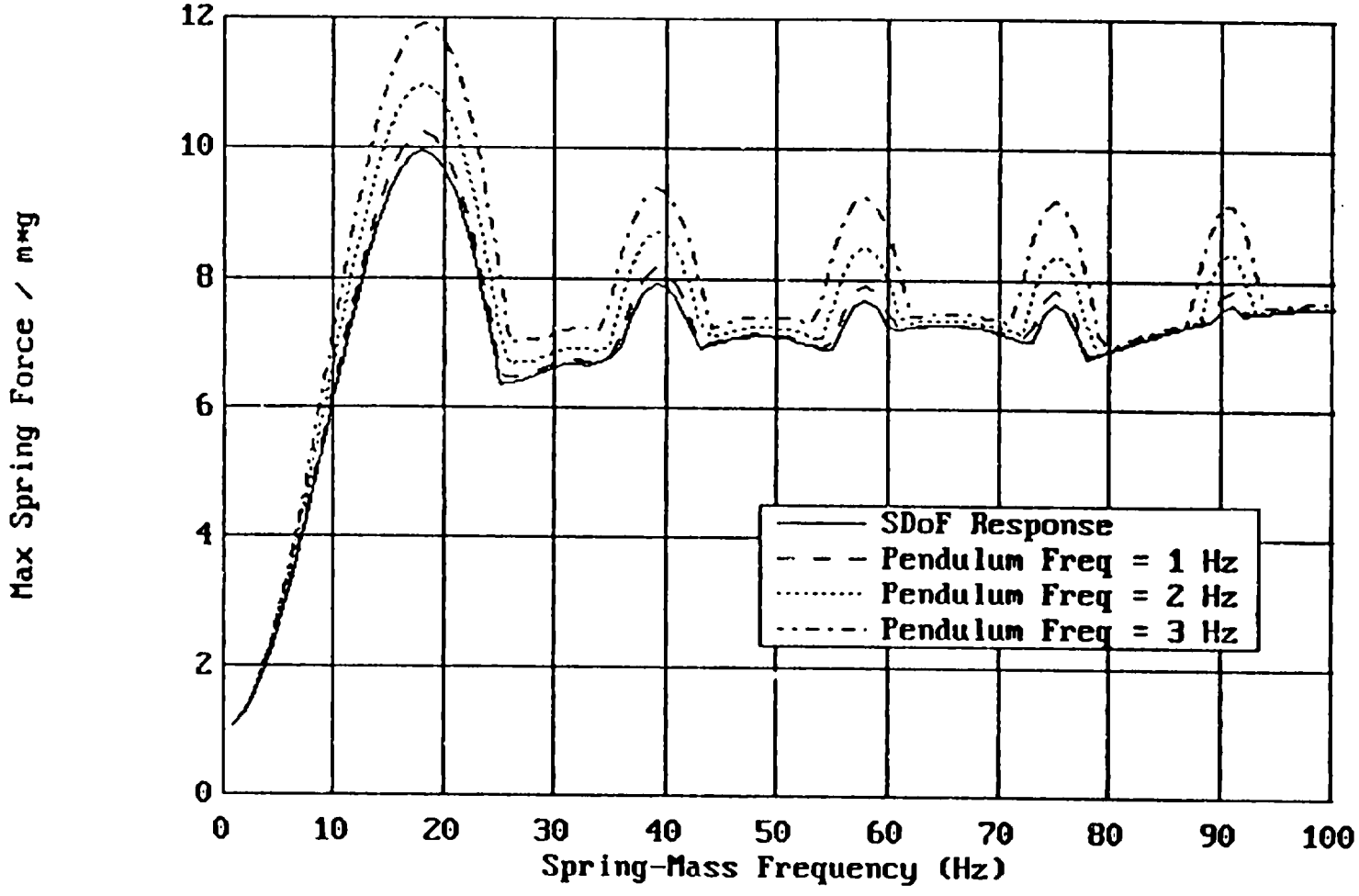

Figure 6. Response of Spring Pendulum to Combined Horizontal and Vertical Support Motion (Base Input: Amplitude = 20 in/sec, Duration = 0.05 sec).

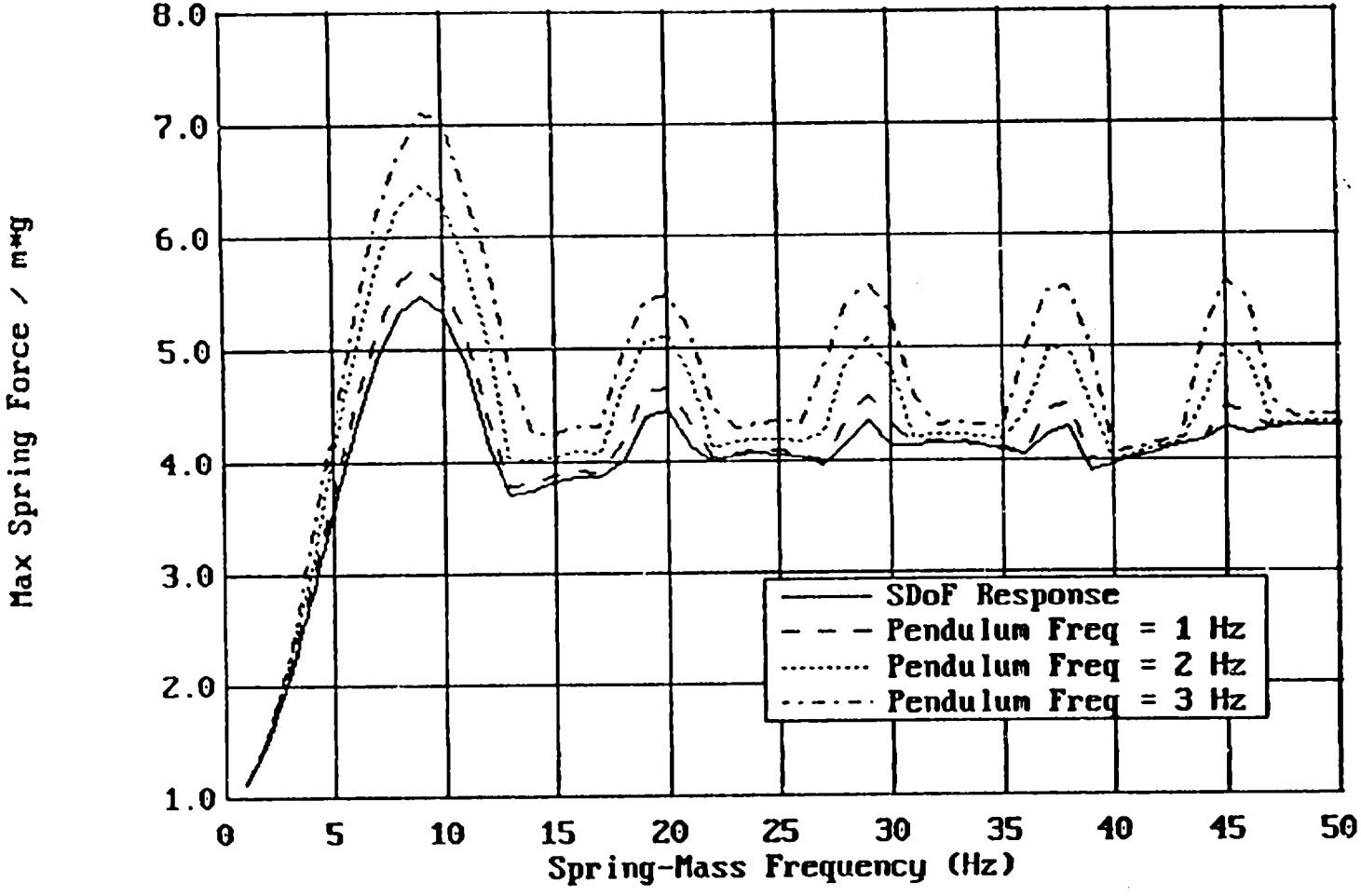

Figure 7. Response of Spring Pendulum to Combined Horizontal and Vertical Support Motion (Base Input: Amplitude = 20 in/sec, Duration = 0.10 sec).

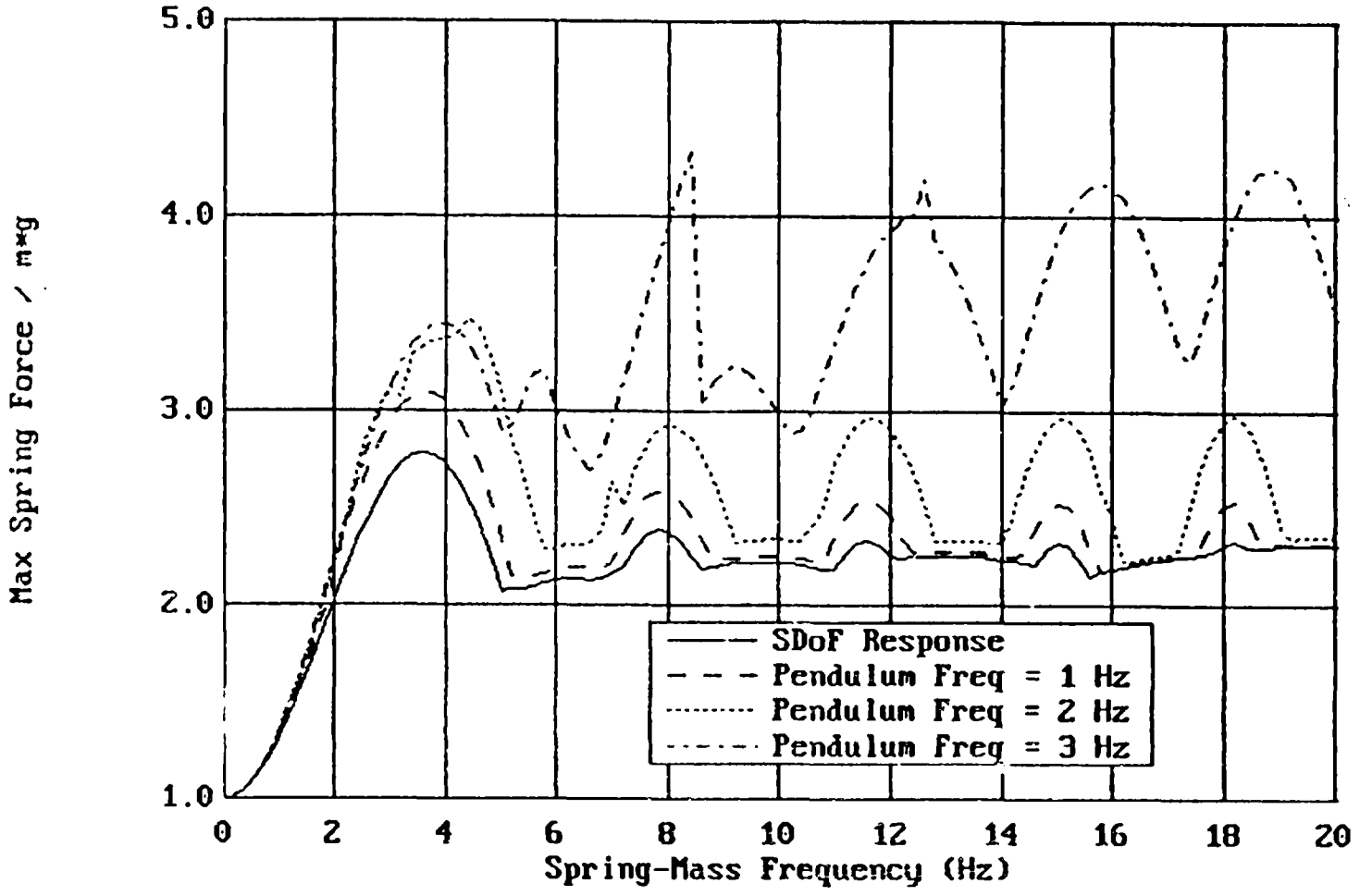

Figure 8. Response of Spring Pendulum to Combined Horizontal and Vertical Support Motion (Base Input: Amplitude = 20 in/sec, Duration = 0.25 sec).

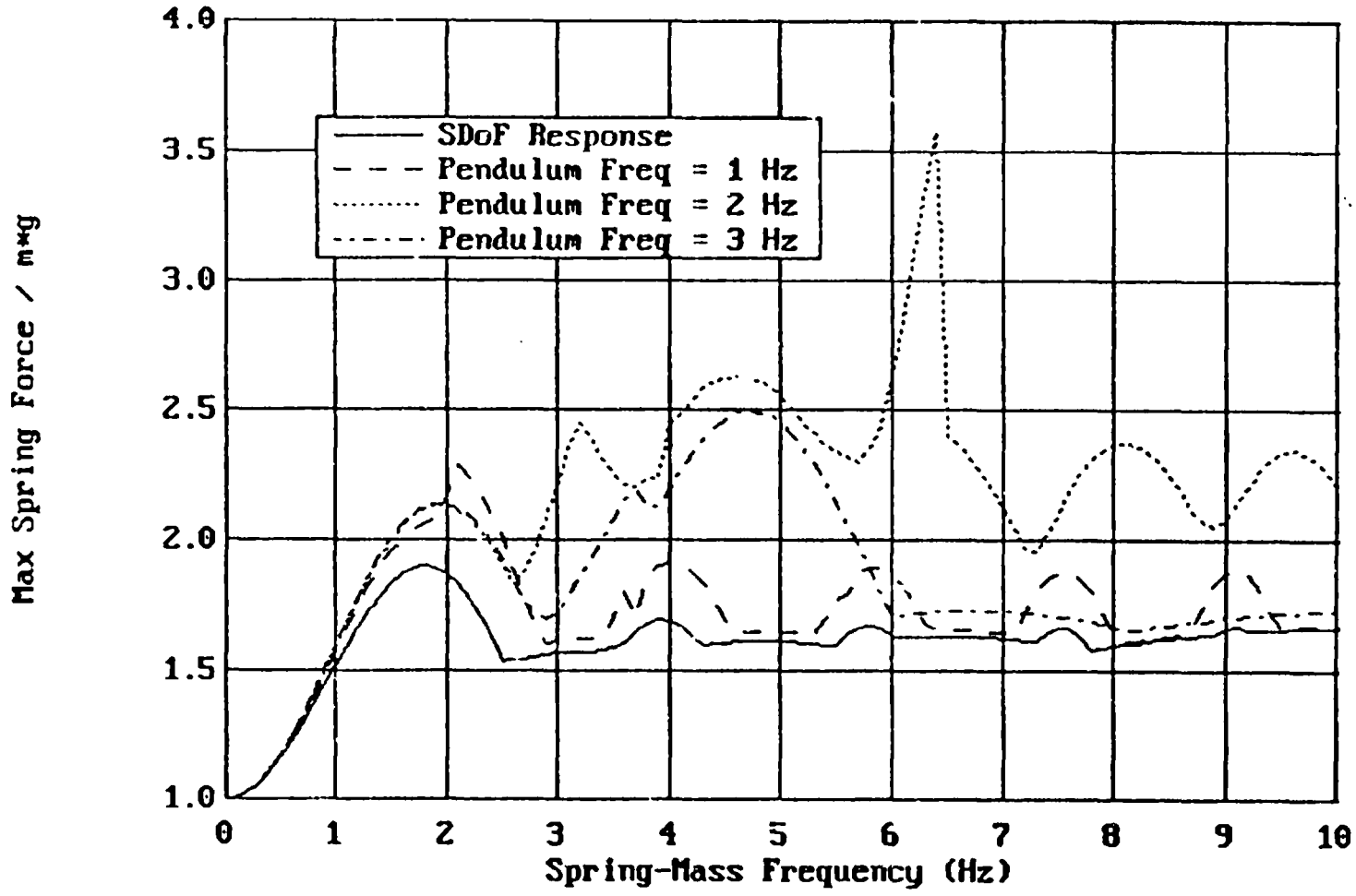

Figure 9. Response of Spring Pendulum to Combined Horizontal and Vertical Support Motion (Base Input: Amplitude = 20 in/sec, Duration = 0.50 sec).

D. EFFECT OF MDOF EQUIPMENT RESPONSE

It is common practice to use the fundamental period (or frequency) of an MDoF system, and enter the shock response spectrum for a given support motion to determine the peak structural response of the system. The contributions to the structural response from higher modes are usually ignored.

To quantify the errors introduced by ignoring higher mode contributions to the structural response, a cantilever beam carrying a tip mass having both translational and rotary inertia was used as a two-dimensional MDoF equipment model. The equipment response was assumed to be linearly elastic. This simple MDoF model is shown in Figure 10. The mass density, cross-sectional area, Young's modulus, moment of inertia, and length of the beam are denoted by ρ, A, E, I, and L, respectively. These parameters were assumed constant throughout the beam. The mass and the radius of gyration of the tip mass are denoted by m and r, respectively.

The derivation of the equation of motion, along with the initial and boundary conditions for this structural system when subjected to support motion are given in Appendix C. The support motion is prescribed as a displacement time-history, $Z(t)$, allowing a velocity jump at time $t = 0$. The relative displacement of the beam with respect to the support is denoted as $u(x,t)$. Based on the principle of linear superposition, the total response of the system can be expressed as the sum of modal contributions via a modal analysis. Due to the orthogonality of different vibration modes, each modal equation of motion can be solved as that for an SDoF system. The derivation of the orthogonality relationship for distinct vibration modes, and the modal equation of motion are also included in Appendix C. Furthermore, the exact solution can be obtained if the support motion can be described by a simple analytical function.

An item of equipment with $k_1 = 1$ and $k_2 = 0.0025$ (refer to Equations (C-51) and (C-52) in Appendix C), is used as an example. The characteristic curve (i.e., the plot of Equation (C-58)) of this system is shown in Figure 11. The roots of this curve are the characteristic values of the free-vibration equation (Equation (C-27)), and the corresponding characteristic functions (obtained from using Equations (C-36), (C-49) and (C-59)) are the free-vibration mode shapes. Although this system has an infinite number of natural vibration modes, only the first seven modes are retained for a modal analysis. The characteristic values of these modes are identified in Figure 11. The normalized mode shapes of the first seven modes are shown in Figures 12 through 18, respectively. The accuracy of the characteristic values and mode shapes deteriorates with higher modes, but fortunately the contributions from higher modes are relatively insignificant.

The support motion (or base acceleration) in this study was modeled as a unit triangular pulse with duration t_d and no rise time. Mathematically, the base acceleration can be expressed as

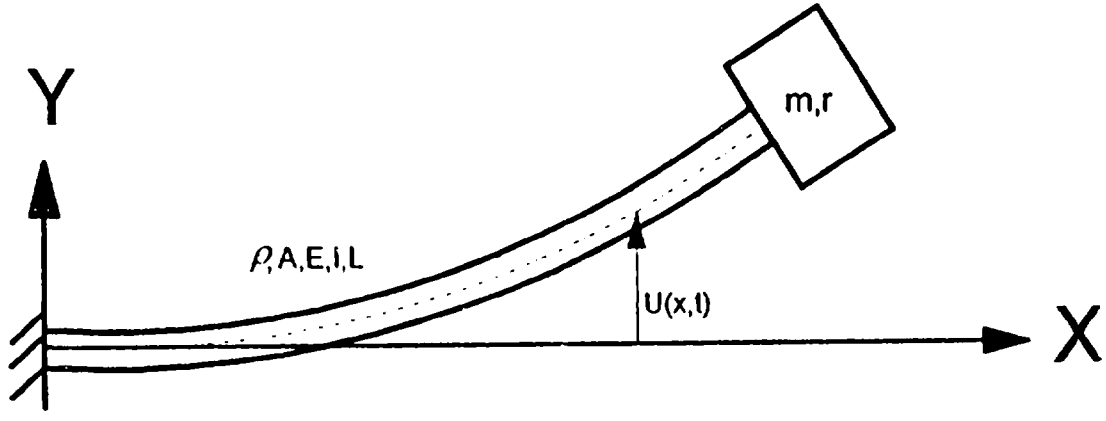

Figure 10. Cantilever Beam Carrying a Tip Mass Having Both Translational and Rotary Inertia

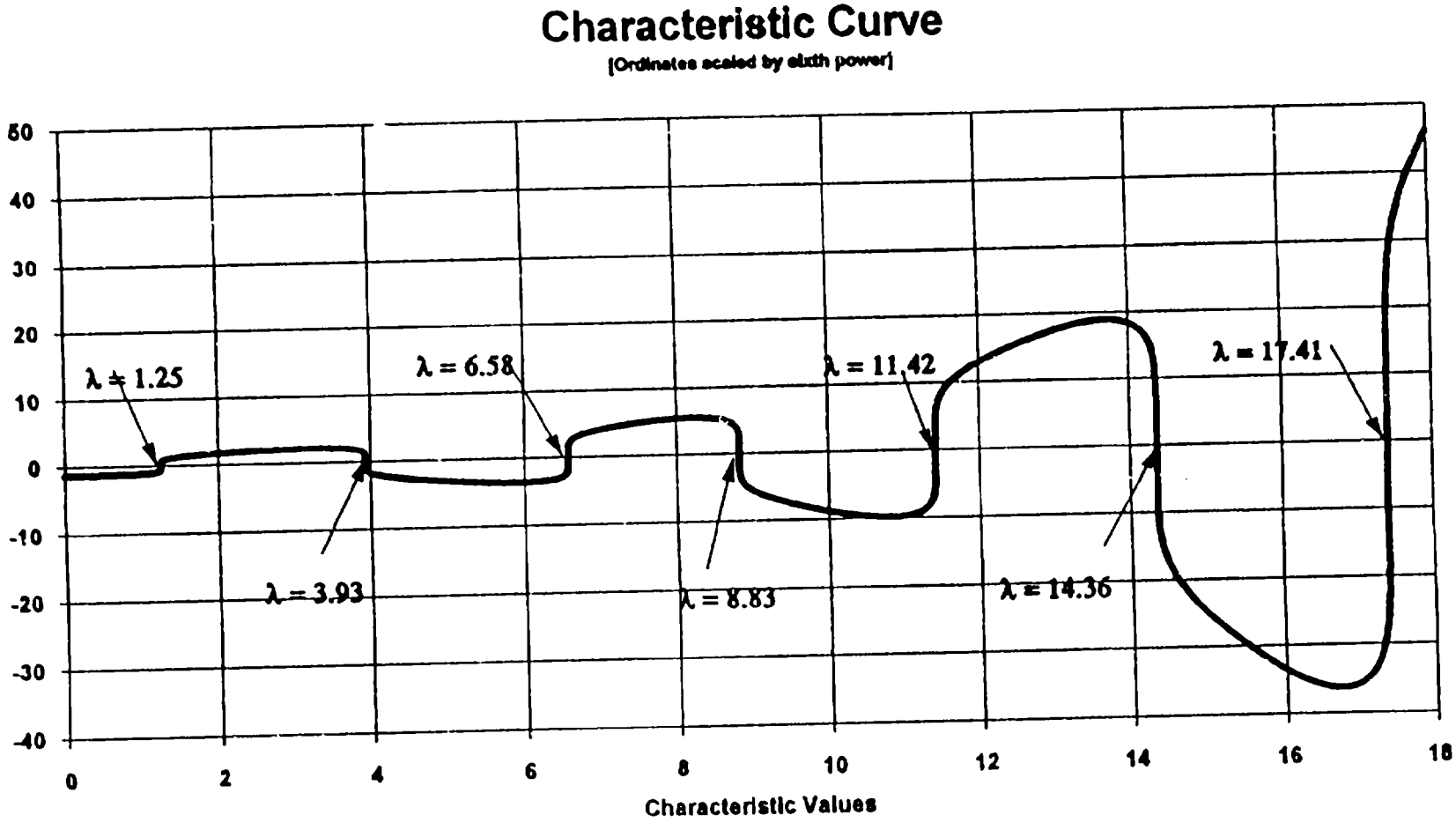

Figure 11. Characteristic Curve

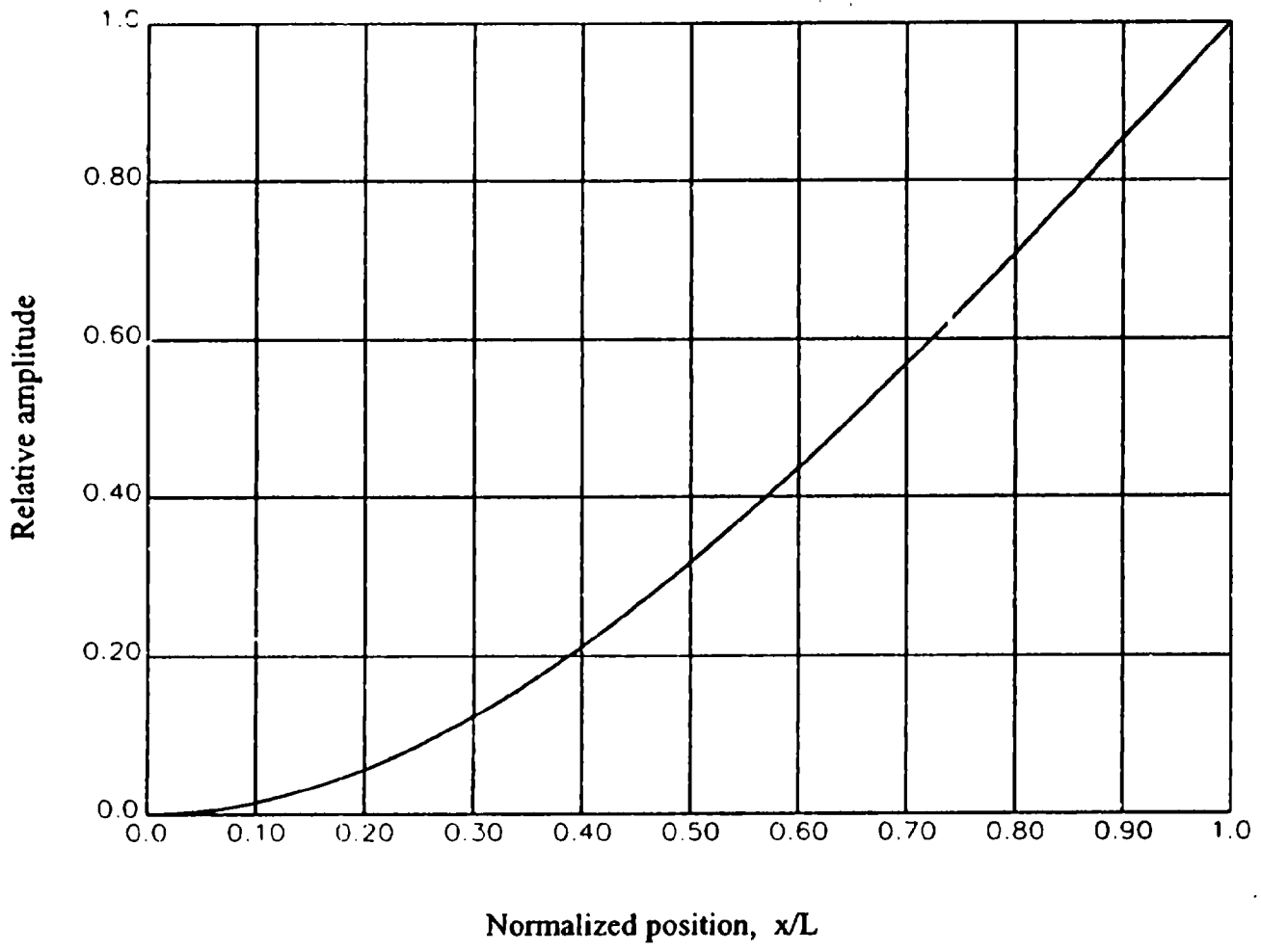

Figure 12. First Mode Shape ($\lambda_1 = 1.247$)

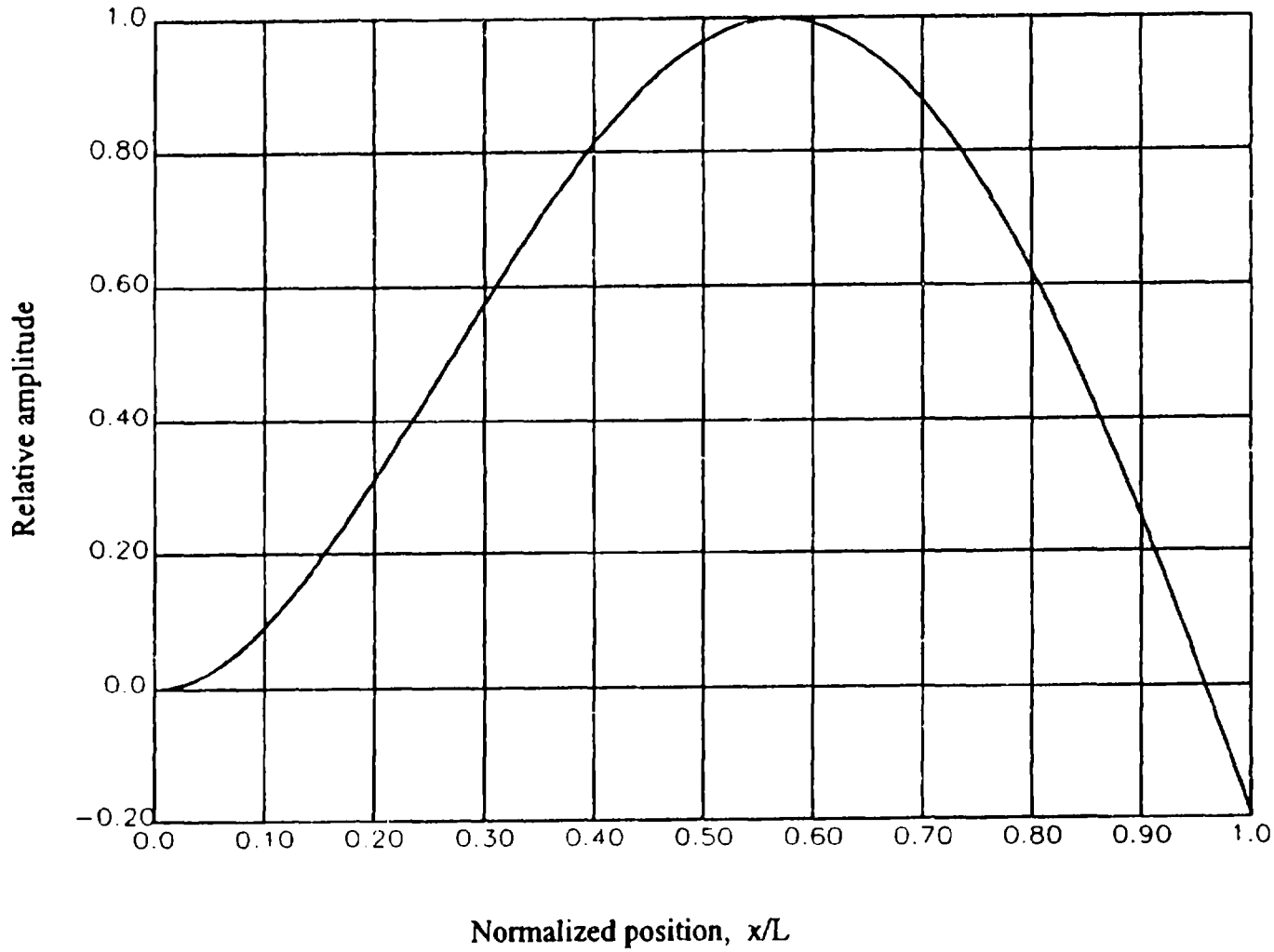

Figure 13. Second Mode Shape (λ_2 = 3.928)

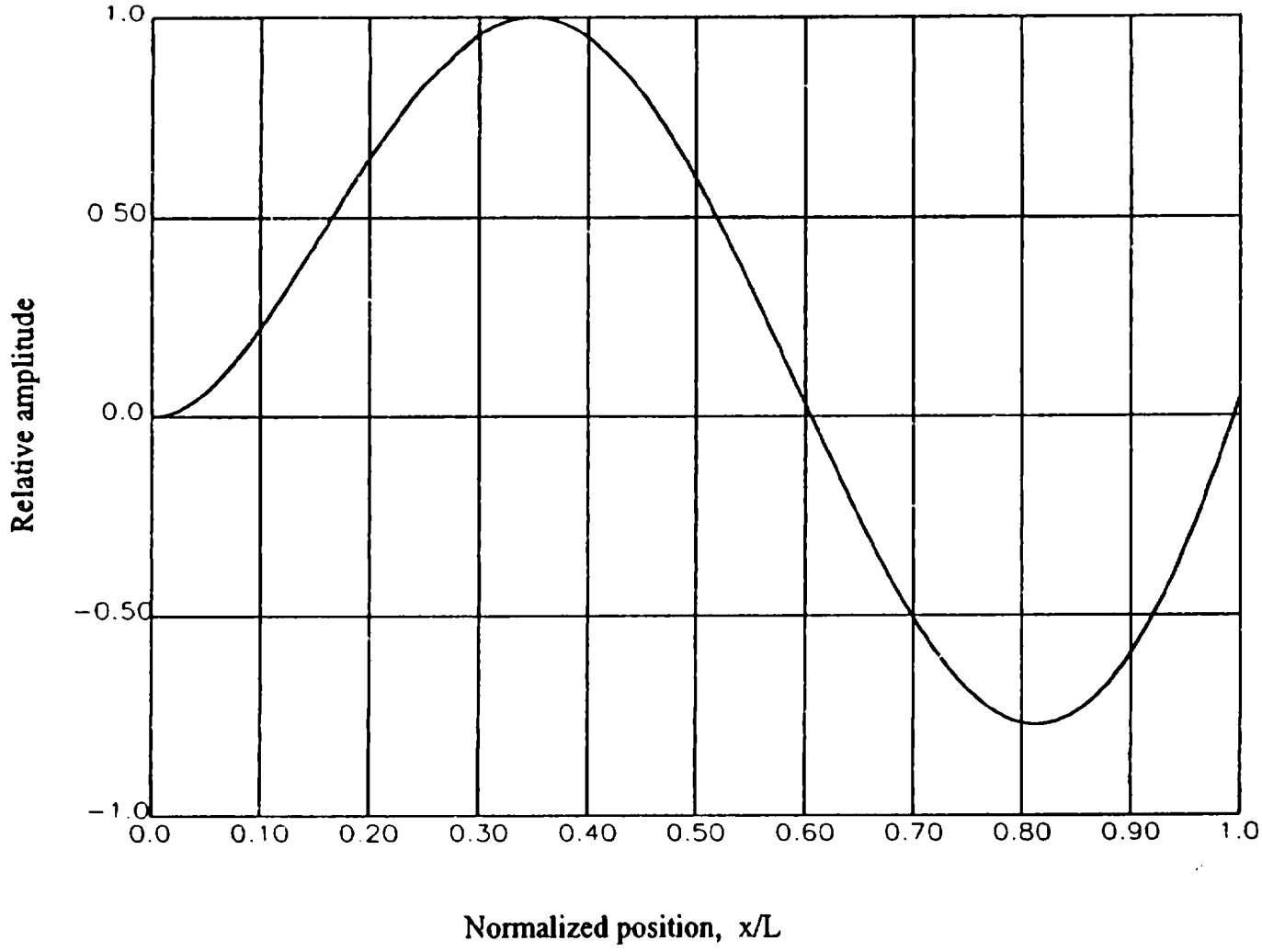

Figure 14. Third Mode Shape (λ_3 = 6.577)

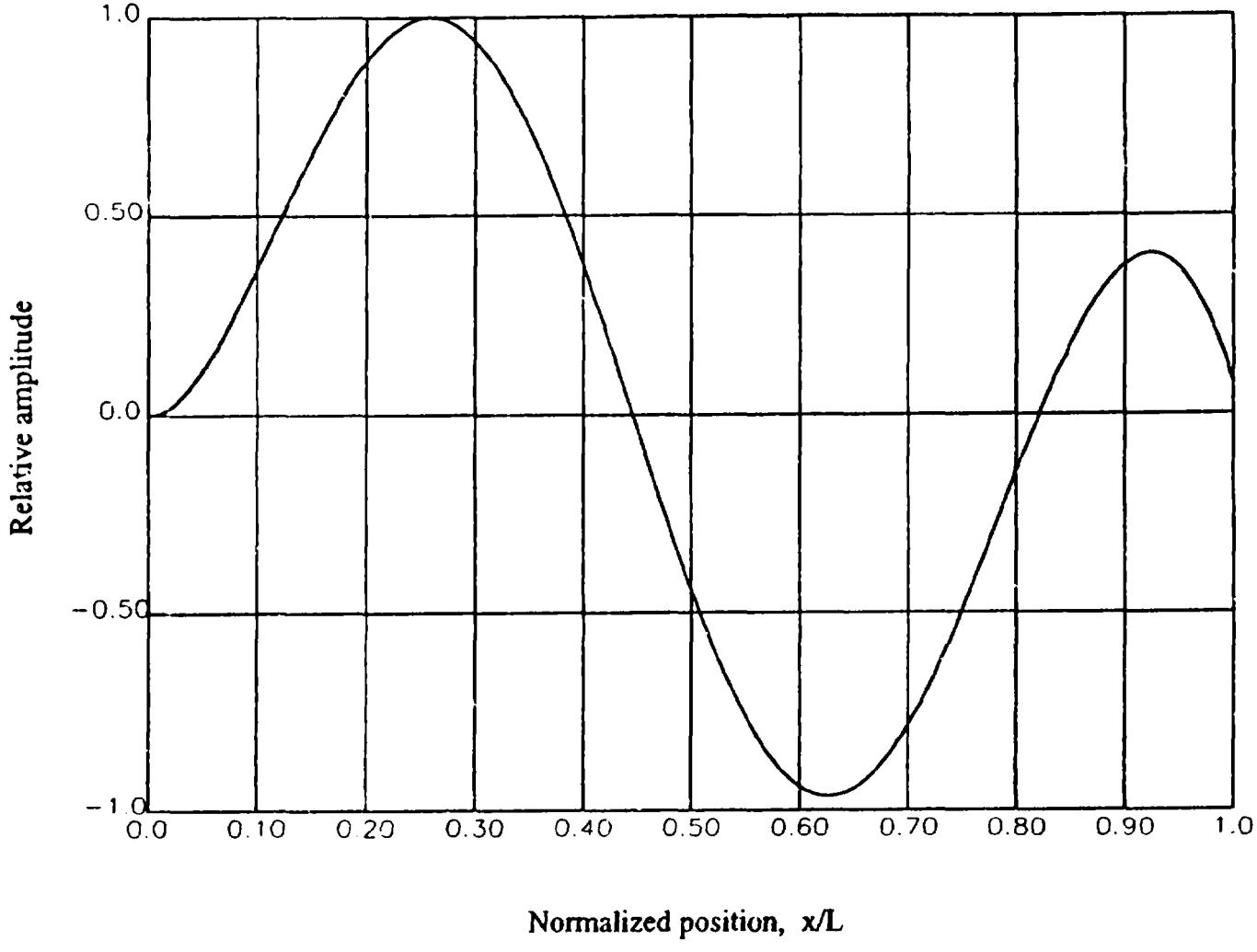

Figure 15. Fourth Mode Shape (λ_4 = 8.832)

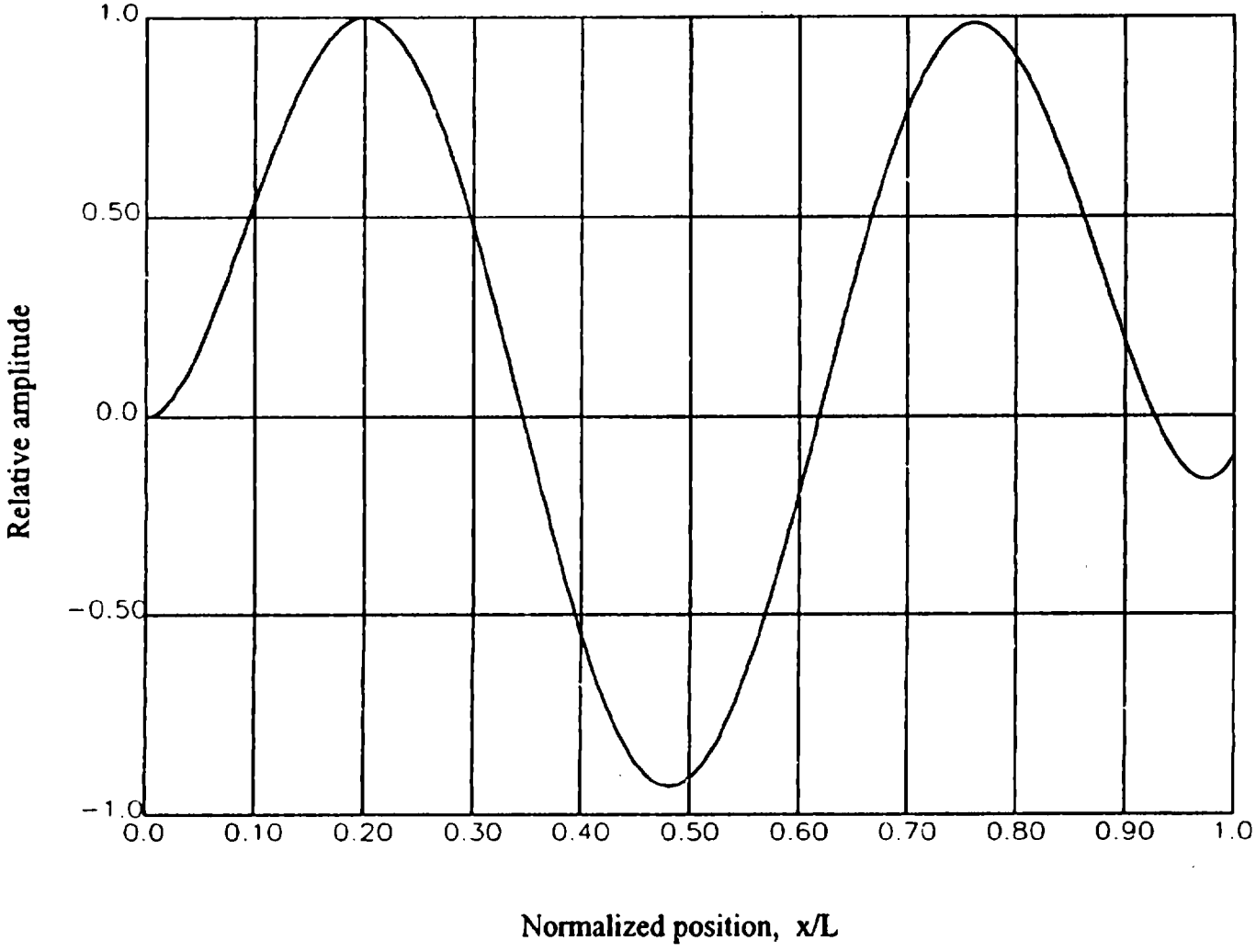

Figure 16. Fifth Mode Shape (λ_5 = 11.417)

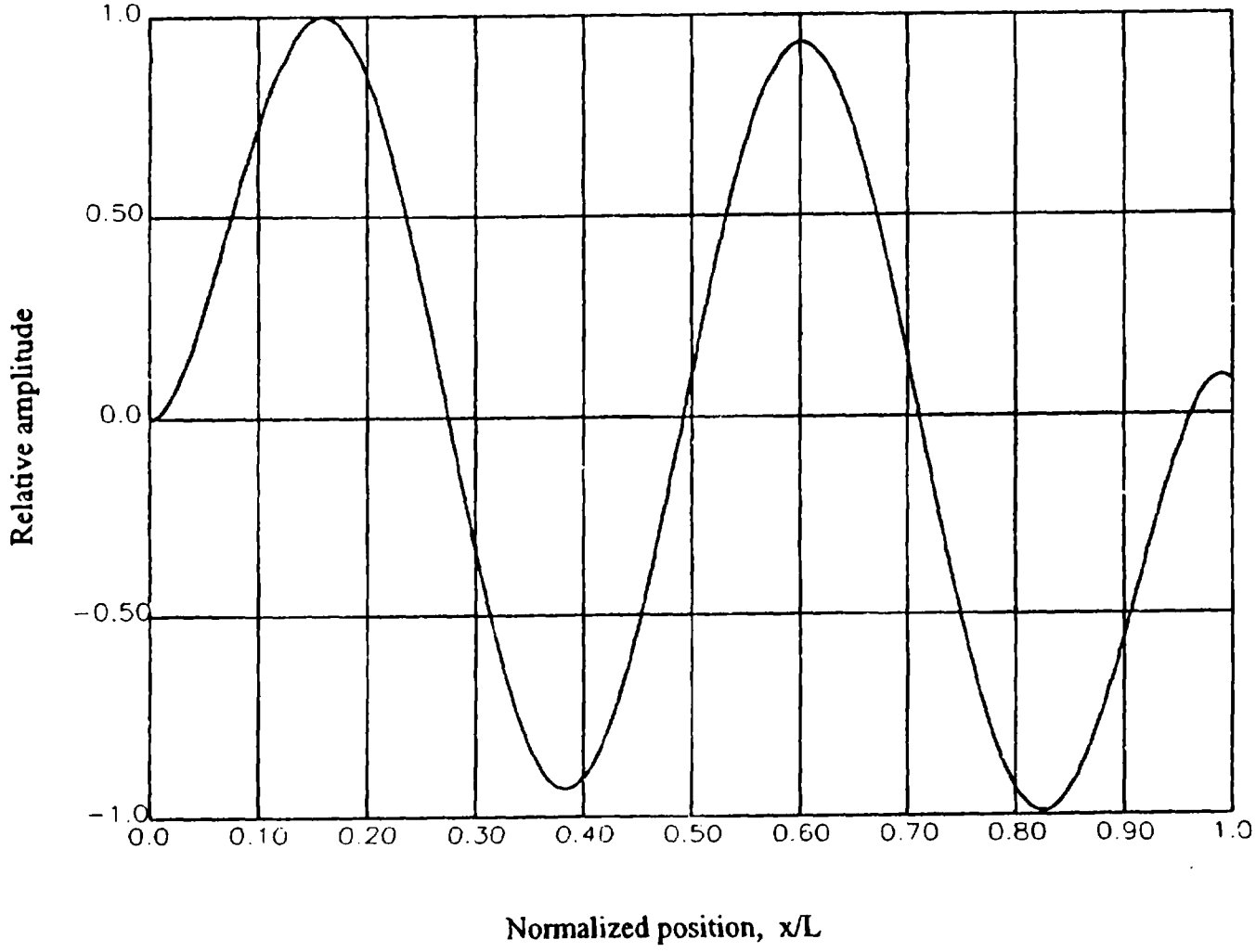

Figure 17. Sixth Mode Shape (λ_6 = 14.355)

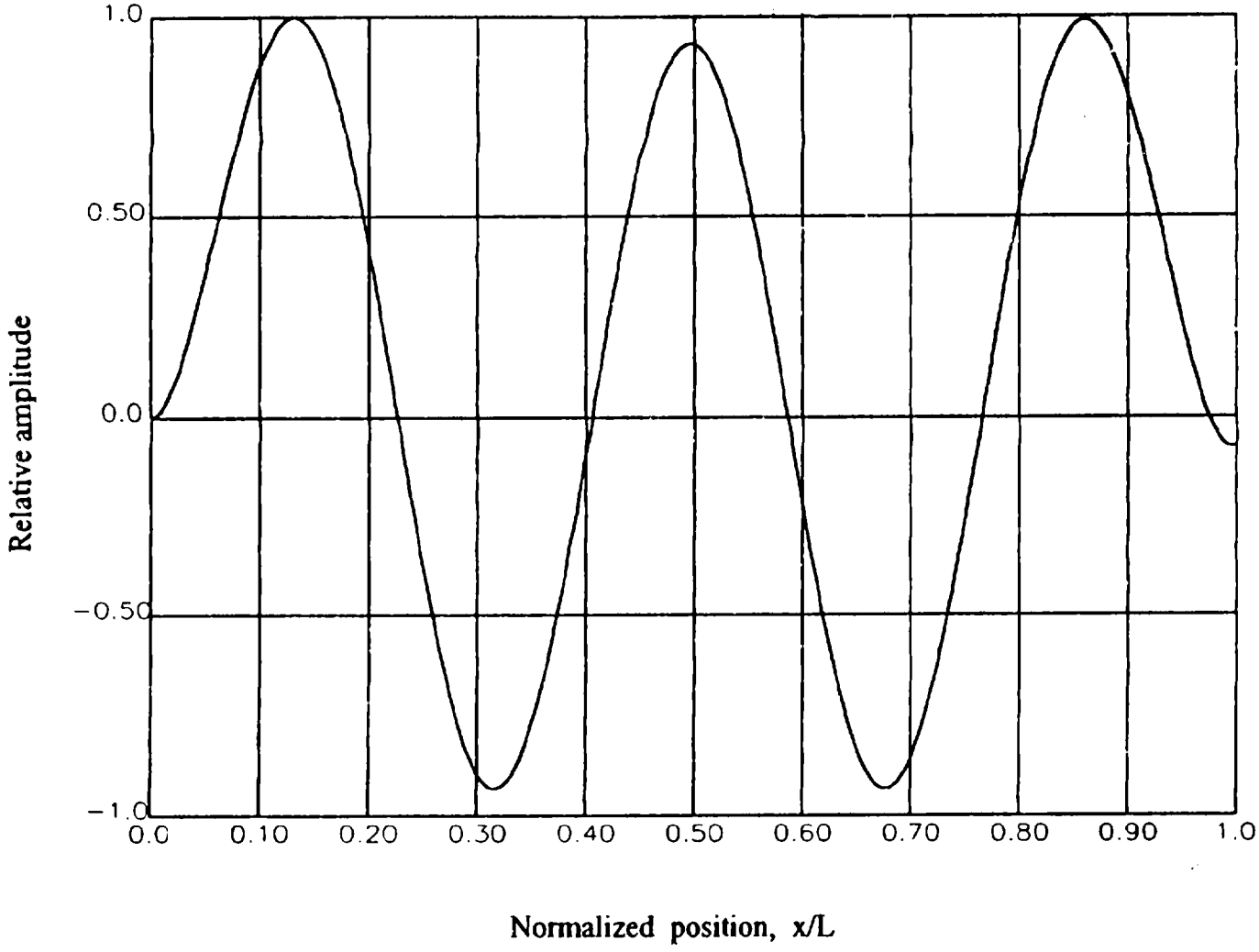

Figure 18. Seventh Mode Shape (λ_7 = 17.414)

$$\bar{\beta}(\psi) = 1 - \frac{\psi}{t_d / T} \tag{8}$$

where T, defined by Equation (C-17) in Appendix C, is the characteristic period of the system. The effects of pulse duration on the equipment response parameters, such as tip mass displacement, base shear, and base moment, were evaluated as functions of t_d / T. The cyclic natural frequency in Hz of the ith mode, f_i, is related to the characteristic period by

$$f_i = \frac{\lambda_i^2}{2\pi T} \tag{9}$$

The characteristic period, T, of the system was assumed to be 0.02 sec in this example. With the characteristic values and mode shapes given, the modal amplitudes, θ_i, for the first seven modes were obtained by directly integrating Equation (C-123). Figure 19 shows the relative displacement time-history of the tip mass for a base motion of duration $2T$, considering MDoF response. The base shear and base moment can be calculated using Equations (C-3) and (C-4), respectively. Figure 20 shows the base shear time-history for a base motion of duration $5T$.

Since the response in each mode is given explicitly, the error of ignoring higher mode contributions can be computed. The error is defined herein as the difference between MDoF(including all seven modes) and SDoF(including the first mode only) values, assuming the total response of the equipment is predominantly in the first mode. The percentage error from using the SDoF model in the calculation of tip displacement, base shear, and base moment is shown as a function of impulse duration in Figure 21. The error increases with the degree of differentiation of the relative displacement with respect to length.

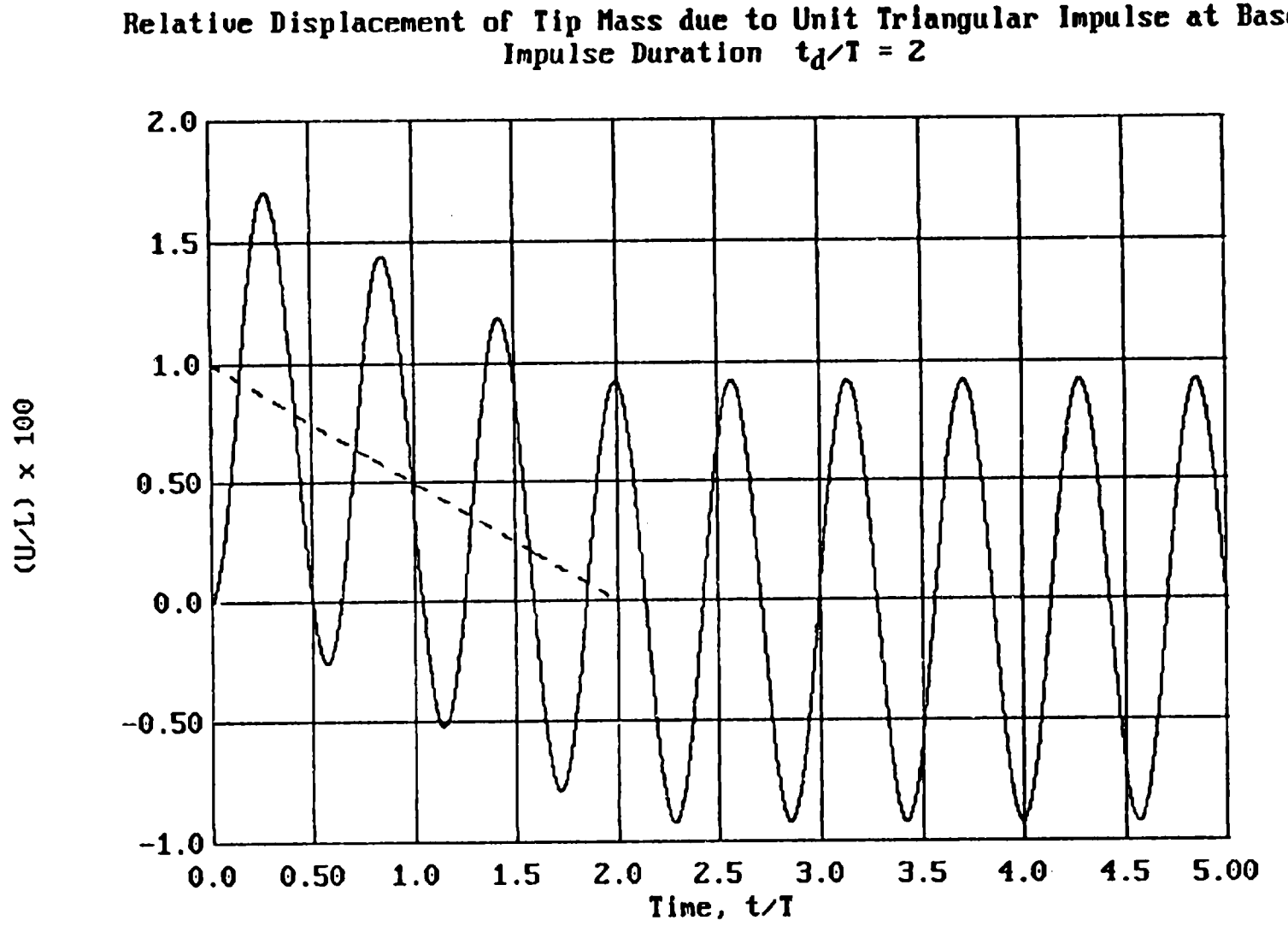

Figure 19. Relative Tip Mass Displacement due to a Unit Triangular Pulse at Base ($t_d / T = 2$)

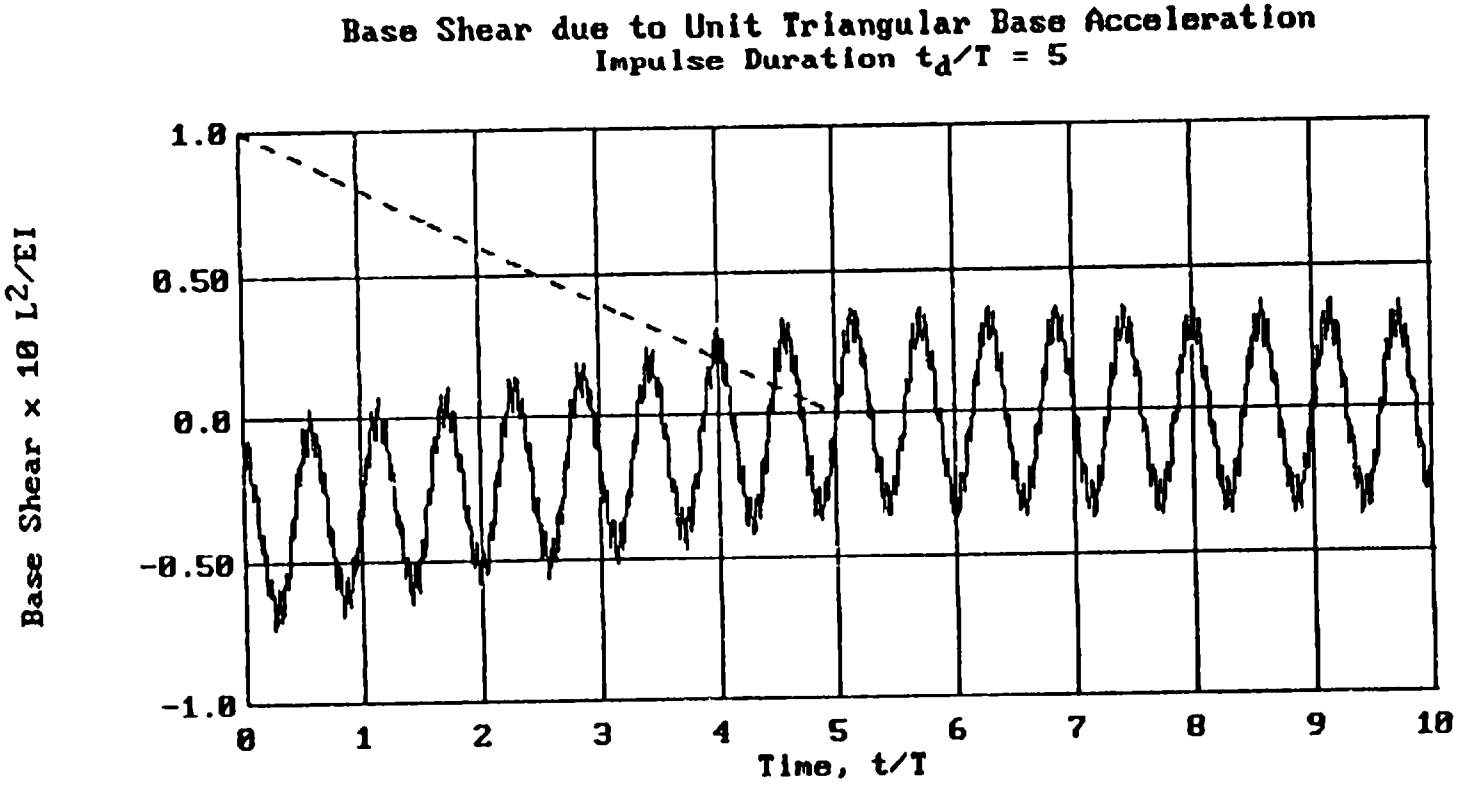

Figure 20. Base Shear due to a Unit Triangular Pulse at Base ($t_d / T = 5$)

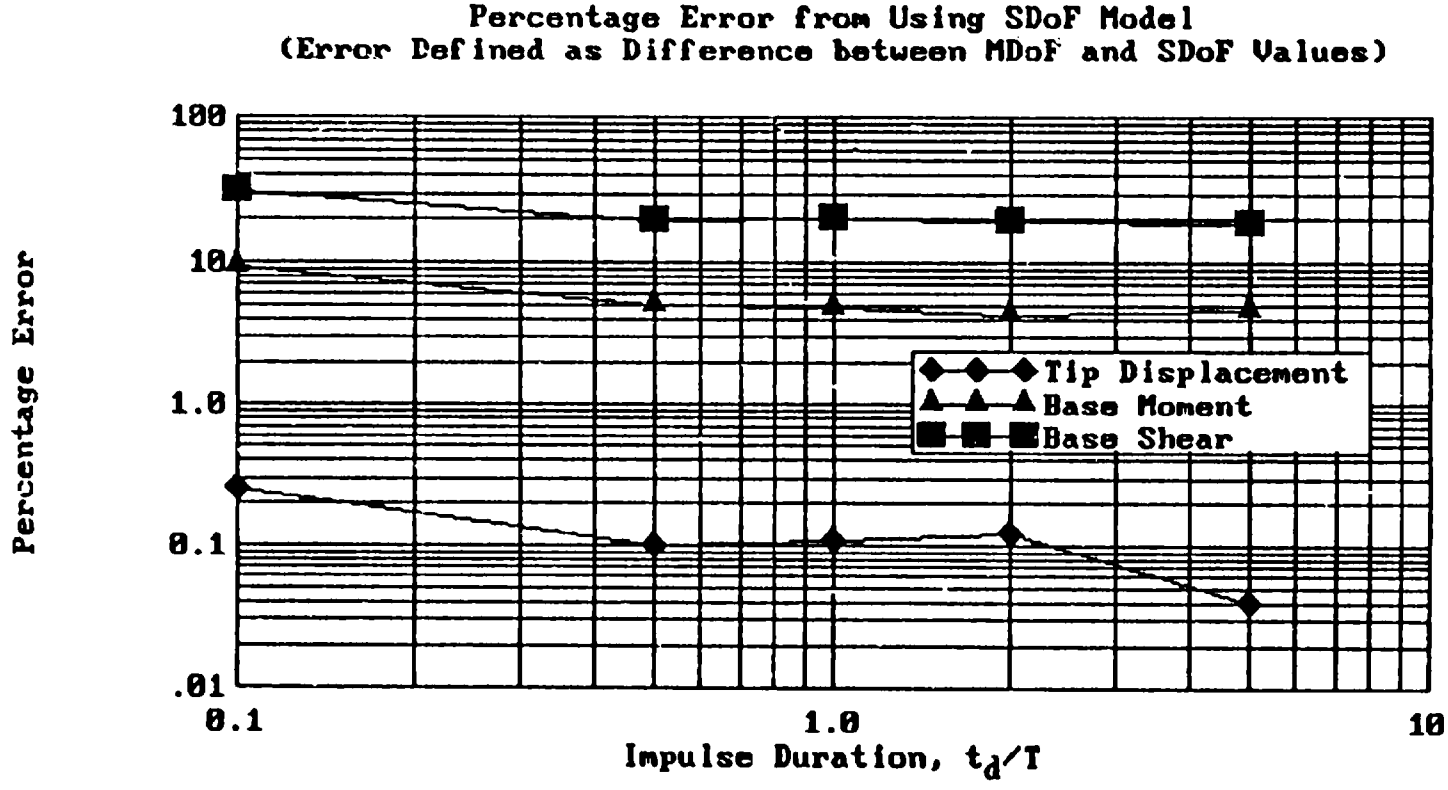

Figure 21. Percentage Error from Using SDoF Model for MDoF Response

SECTION IV

CONCLUSIONS AND RECOMMENDATIONS

A. CONCLUSIONS

The objective of this study was to investigate the errors associated with characterizing the shock tolerance of equipment via the classic, linear, SDoF shock response spectrum. Two simple mathematical equipment models were developed for the investigation: (1) a spring pendulum, which possesses two degrees of freedom and geometric nonlinearity, and (2) a clamped beam carrying a tip mass having both translational and rotary inertia, which possesses an infinite number of linear, orthogonal modes. These models were used to investigate and quantify the effect of factors such as: waveform dependency of equipment shock response; multi-degree-of-freedom (MDoF) vs. SDoF equipment response; the effect of multidirectional loading on equipment response; and the effect of geometric nonlinearity on equipment response.

This study uncovered and quantified several shortcomings of the SRS approach to characterizing equipment shock tolerance:

- It was proven that SRS-based fragility spectra are not unique. Even for an equipment item which can be modeled by a simple SDoF undamped oscillator, different base excitations generally produce different fragility spectra.
- The spring pendulum model was used to illustrate the response of a geometrically nonlinear item of equipment to two-dimensional base motion. It was shown that extremely erratic behavior is possible if the frequency of the base motion approaches one of the natural frequencies of the equipment model. The maximum response can be several times greater than that of a simple SDoF oscillator.
- The cantilever beam model was used to show that the maximum repsonse of an MDoF system will always exceed the response of a simple oscillator.

In conclusion, this study has proven the inadequacy of the linear, SDoF shock response spectrum for characterizing the shock tolerance of equipment. Complex, nonlinear mechanical equipment subjected to multidirectional support motion is often not adequately represented by an SDoF model.

B. RECOMMENDATIONS

Based on the results of this study, a more rigorous approach for assessing equipment shock tolerance is required. The following points should be kept in mind while developing this new procedure:

- When an equipment item is tested to determine its shock tolerance, the test input waveform must be representative of the anticipated threat input waveform. Multidirectional support motion must be reproduced. Equipment tests should excite the same response modes, and produce the same failure modes, as the actual in-service base motion.
- Analytical equipment models must be detailed enough to reproduce the salient features of the actual equipment response. The model need not encompass the entire item of equipment, but it must adequately represent the critical components. The input motion to the model must mimic the in-service motion.

SECTION V

REFERENCES

Department of the Army, Fundamentals of Protective Design for Conventional Weapons, Technical Manual No. 5-855-1, Headquarters, Department of the Army, Washington DC, 3 November 1986.

Drake, J.L., Twisdale, L.A., Frank, R.A., Dass, W.C., Rochefort, M.A., Walker, R.E., Britt, J.R., Murphy, C.E., Slawson, T.R., and Sues, R.H., Protective Construction Design Manual, Report No. ESL-TR-87-57, Air Force Engineering & Services Center, Engineering & Services Laboratory, Tyndall Air Force Base, FL, November 1989.

Kiger, S.A., Balsara, J.P., and Baylot, J.T., "A Computational Procedure for Peak Instructure Motions and Shock Spectra for Conventional Weapons," The Shock and Vibration Bulletin, No. 54, June 1984.

Blume, J.A., Newmark, N.M., and Corning, L.H., Design of Multistory Reinforced Concrete Buildings for Earthquake Motions, Portland Cement Association, 1961; updated as Ghosh, S.K. and Domel, A.W., Jr., Design of Concrete Building for Earthquake and Wind Forces, Portland Cement Association and International Conference of Building Officials,1992; see also Paz, M., Structural Dynamics / Theory and Computation, Van Nostrand Reinhold Company Inc., New York, 1985.

BIBLIOGRAPHY

American Standard Specification for Design, Construction and Operation of a Variable Duration, Medium Impact Shock Testing Machine for Lightweight Equipment, ASA Publication S2.1, (1961).

American Standard Specification for Design, Construction and Operation of Class H1 (High Impact) Shock Testing Machines for Lightweight Equipment, ASA Publication Z24.17, (1955).

Anon, A Study of the Determination of the Internal Impedance of a Machine, A.D. Little, Inc., (July 1961), 55 pp., ASTIA #265995.

Anon, "Shock and Vibration Test Equipment," Electro-Technol., Vol 69, (February 1962), pp. 233-234, 236, 238, 240.

Anon, Code of Equipment Design Practice, Technical Progress Statement No. 3, Contract No. NU/C/345/GSIA, EPS, Lts., Sitting Bourne Kent, (no date).

ASTM Standards, Part 7, (1955), p. 1087.

ASTM Standards, "Shock Testing Mechanism for Electrical Indicating Instruments," ASA Publication C39.3-1948, Part7, (1955), p. 1101.

Belsheim, R.O., G.J. O'Hara, and A.F. Dick, "Shock Design Analysis of Shipboard Machinery and Equipment," Shock, Vibration and Associated Environments, Bulletin No. 28, Part I, (July 1960), p. 130.

Biot, M.A., "Theory of Vibration of Buildings During Earthquake" (in English), Zeitschrift fur Angewandt Mathematik und Mechanik, Band 14, Heft 4, (August 1934).

Biot, M.A., Transient Oscillations in Elastic Systems, Ph.D. thesis, California Institute of Technology, (1932).

Blake, R.E., R.O. Belsheim, and J.P. Walsh, "Damaging Potential of Shock and Vibration," Shock and Vibration Instrumentation, ASME, (1956).

Brodd, R.J., and W.G. Eicke, Jr. "Effect of Vibration and Shock on Unsaturated Standard Cells," J. Rsch., NBS, Vol 66C, (April/June 1962), pp. 85-97.

Bush, V., Operational Circuit Analysis, Wiley, (1937).

Carson, John E., Electric Circuit Theory and Operational Calculus, McGraw-Hill, (1926).

Cauthen, L.J., "The Effects of Seismic Waves on Structures and Other Facilities," Engineering with Nuclear Explosives, Proc., 3rd Plowshare Symposium, AEC TID-7695, (1964), pp. 207-228.

Chapman, C.W., "Dynamic Loading and Some Indications of Its Effect on Internal Combustion Engines," Proc. Inst. Mech. Eng., (London), Vol 153, (1945), pp. 221-236.

Chew, R.S., "Effect of Earthquake Shock on High Buildings," ASCE Proceedings, Vol. 34, No. 1, (Jan 1908), pp. 8-15; discussion Vol. 34 No. 3, (Mar 1908), pp. 292-296; discussion Vol. 34, No. 4, (Apr 1908), pp. 391-393.

Crandell, F.J., "Ground Vibration Due to Construction Blasting and its Effects Upon Structures," J. BSCE, (April 1949), pp. 222-245.

Crawford, R.E., C.J. Higgins, and E.H. Bultmann, Jr., A Guide for the Design of Shock Isolation Systems for Ballistic Missile Defense Facilities, Mechanics Research, Inc., Civil/Nuclear Systems Division final report to the U.S. Army Construction Engineering Research Laboratory, Champaign, Illinois, CERL-TR-S-23, (August 1973).

Crede, C.E., "Concepts in Shock Testing Equipment," Colloquim on Shock and Structural Response, ASME, (August 1960).

Crede, C.E., "How to Evaluate Shock Tests," Machine Design, (December 1951).

Crede, C.E., "Shock Testing of Airborne Electronic Equipment," Tele-Tech Mag., (July/August 1951).

Crede, C.E., "The Role of Shock Testing Machines in Design," Mechanical Engineering, (July 1954), pp. 564-567.

Crede, C.E., "The Simulation of Shock and Vibration Environments," Proceedings, Society for Experimental Stress Analysis, Vol XVII, No. 1, (1957).

Crede, C.E., Unpublished Data from Tests Conducted at the California Institute of Technology, (1962).

Crede, C.E., and M.C., Junger, "Designing for Shock Resistance," Machine Design, (December 1950), Parts I and II.

Crede, C.E., and M.C. Junger, A Guide for Design of Shock Resistant Naval Equipment, U.S. Bureau of Ships, NAVSHIPS 250-660-30, (1949).

Crede, C.E., and E.J. Lunney, Establishment of Vibration and Shock Tests for Missile Electronics as Derived from the Measured Environment, WADC TR 56-503, (1 December 1956), ASTIA Document No. AD 118133.

Criner, H.E., G.D. McCann, and C.E. Warren, "A New Device for the Solution of Transient Vibration Problems by the Method of Electrical-Mechanical Analogy," ASME JAM, Vol. 12, No. 3, (1945), pp. A-135 to A-141.

D'Agostino, Robert, "Selecting Threaded Fasteners for Shock Loads," Machine Design, Vol 35, No 4, (February 1963), p. 169-171.

Dick, A.F., Reed-Gage Shock-Spectrum Characteristics of Navy Light-Weight High Impact Shock Machine, NRL Report 4749.

Dick, A.F., and R.E. Blake, Reed-Gage Shock-Spectrum Characteristics of Navy Medium-Weight High Impact Shock Machine, NRL Report 4750.

Dove, R.C., Evaluation of In-Structure Shock Prediction Techniques for Buried Structures, U.S. Army Corps of Engineers Waterways Experiment Station, Technical Report SL-91-20, (October 1991).

Fischer, E.G., "Design of Equipment to Withstand Underground Shock Environments," Shock, Vibration and Associated Environments, Bulletin No. 28, Part I, (July 1960), p. 75.

Gardner, M.F., and J.L. Barnes, Transients in Linear Systems, Vol. 1, Wiley, (1942); Vol 2 was never published.

Granath, J.A., and C.A. Miller, "Response of Electronic Equipment to Nuclear Blast," Shock, Vibration and Associated Environments, Bulletin No. 29, Part II, (March 1961).

Green, J.H., "The Response of Missile Components to Water-Entry Shock," Symposium on Shock, Vibration & Associated Environments, Bulletin No. 26, (December 1958).

Gupta, A.K., Response Spectrum Method in Seismic Analysis and Design of Structures, Blackwell Scientific Publications, (1990).

Heaviside, O., Electrical Papers, Macmillan, (1892).

Heaviside, O., Electromagnetic Theory, Vol. 1 (1893), Vol. 2 (1899), Vol. 3 (1912), Van Nostrand.

Housner, G.W., An Investigation of the Effects of Earthquakes on Buildings, Ph.D. thesis, California Institute of Technology, (1941).

Housner, G.W., and P.C. Jennings, Earthquake Design Criteria, Earthquake Engineering Research Institute Monograph Series, (1982).

Jacobsen, R.H., and M.B. Levine, "Effects of Shock and Vibration Environment on Electronic Equipment," Shock and Vibration, Bulletin No. 22, (July 1955), p. 93.

Kennard, D.C., and I. Vigness, "Shock Testing Machines and Procedures," Shock and Vibration Instrumentation, ASME, (1956).

Kornhauser, M., "Prediction and Evaluation of Sensitivity to Transient Accelerations," ASME Journal of Applied Mechanics, Vol 21, No 4, (1954), pp. 371-380.

Levin, Alexander, "Shock Hardening Electronic Equipment," Buships J., 12:14, (February 1963).

Lowe, R., Barry Shock and Vibration Control Notes, No 7, Barry Controls, Inc., Watertown, Mass, (August 1957).

Luhrs, H.N., and H.R. Spence, Influence of Shock Machine Loading on Shock Spectra, STL Report 7103-00 18 NU 000, AFBMD TN 61-31, (May 1961), 11 pp, ASTIA Doc #260308.

Lunney, E.J., and C.E., Crede, The Establishment of Vibration and Shock Tests for Airborne Electronics, WADC TR 57-15, (July 1958), ASTIA Document No. AD 142349.

MacDuff, J.N., and S.R. Curreri, Vibration Control, Chapter 7, McGraw-Hill Book Company, Inc., New York, (1958).

Marquis, J.P., and D. Morrison, "Equipment Qualification Procedures and Fragility Data," Chapter 12, Section 8 in the Defense Nuclear Agency C.W.E. Handbook, draft, (October 1991).

Matlock, H., E.A. Ripperberger, J. Turnbow, and J.N. Thompson, "Drop-Test Facilities and Instrumentation," Shock and Vibration Bulletin, No 25, Part II, Page 144, Office of the Secretary of Defense R&D, (December 1957).

Military Specifications for Electron Tubes, MIL-E-1B (Sec. 4.9.20.5), Armed Services Electro Standards Agency, Fort Monmouth, New Jersey, (2 May 1952).

Military Specification for Shock Proof Equipment MIL-S-901B (Navy), (9 April 1954), or Interim Military Specification Tests, Shock, Vibration, and Inclination, MIL-T-17113 (Ships), (25 July 1952).

Mindlin, R.D., "Dynamics of Package Cushioning," Bell System Technical Journal, Vol. 24, Nos. 3-4, (Jul-Oct 1945), pp. 353-461; reprinted as Monograph B-1369.

Newmark, N.M., and W.J. Hall, Earthquake Spectra and Design, Earthquake Engineering Research Institute Monograph Series, (1982).

Nahin, P.J., "Oliver Heaviside," Scientific American, Vol. 262, No. 6, (June 1990), pp. 122-129.

Novoselov, V.S., "Impact Testing of Measuring Instruments," Leningrad State University, Izvestiya vysshikh uchebnykh zavedeniy, Priborostr Oye Niye, Vol 5, No 3, (1962), pp. 141-149; S/146/62/005/003, A.I.D. Press No 791, (12 September 1962).

Parfitt, G.G., and J.C. Snowdon, "Incidence and Prevention of Damage due to Mechanical Shock," J. Acoust. Soc. Am., Vol 34, (April 1962), pp. 462-468.

The Hyge Shock Tester, Bulletin 4-70, Consolidated Electrodynamics Corp., Rochester, New York, (February 1957).

The Ralph M. Parsons Company, et. al., A Guide for the Design of Shock Isolation Systems for Underground Protective Structures, Final Report to the Structures Branch, Research Directorate, Air Force Special Weapons Center, Kirtland Air Force Base, New Mexico, SWC TDR 62-64, (December 1962).

U.S. Military Specification MIL-S-4456, or U.S. Air Force Specification 7201.

Van der Pol, B., and H. Bremmer, Operational Calculus, Cambridge University Press, (1964).

Vigness, I., "The Fundamental Nature of Shock and Vibration," Electrical Manufacturing, (June 1959).

Vigness, I., "Shock Testing Machines," Shock and Vibration Handbook, Vol 2, Ch 26, McGraw-Hill Book Company, Inc., New York, (1961).

Wood, J.D., "Factors Affecting the Response of Missiles Excited by Ground Shock," Shock, Vibration and Associated Environments, Bulletin No. 28, Part III, (September 1960).

Woodward, K.E., Damages Resulting from Laboratory Vibrations and High Impact Shock Tests, USNRL Report 4179, (September 1953).

Zorowski, C.F., "Reduction of Shock Transmission by Equipment Damping," Appl. Sci. Res., Vol II, (1962), pp. 53-64.

This page is left blank

APPENDIX A

DYNAMIC RESPONSE OF A SPRING PENDULUM TO SUPPORT MOTION

Dynamic Response of a Spring Pendulum to Support Motion

Consider the response of the spring pendulum shown below, to support motion.

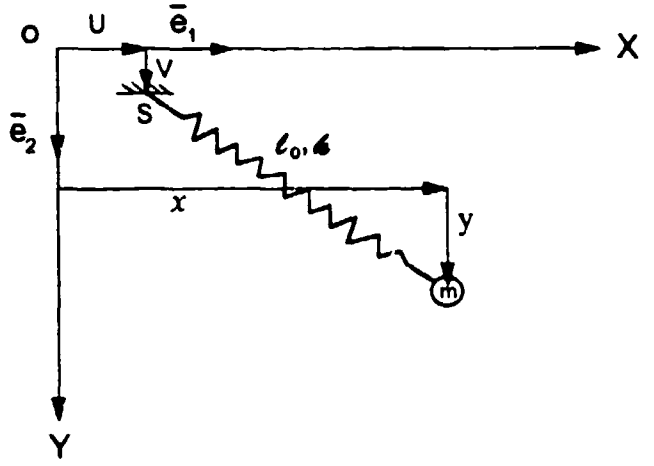

The position vector of the support point, S, is

$$\bar{r} = u\bar{e}_1 + v\bar{e}_2 \tag{A-1}$$

and the position vector of the suspended mass, m, is

$$\bar{R} = x\bar{e}_1 + (l_0 + y)\bar{e}_2 \tag{A-2}$$

where

l_0 = unstretched spring length

u = X-displacement of the support

v = Y-displacement of the support

x = X-displacement of m from the undeformed position

y = Y-displacement of m from the undeformed position

The spring vector is

$$\bar{R} - \bar{r} = (x-u)\bar{e}_1 + [l_0 + (y-v)]\bar{e}_2 \tag{A-3}$$

so that the spring length is

$$l = \sqrt{(\bar{R}-\bar{r})\cdot(\bar{R}-\bar{r})} = \sqrt{(x-u)^2 + [l_0 + (y-v)]^2} \tag{A-4}$$

and a unit vector pointing along the spring from support to mass is

$$\bar{n} = \frac{\bar{R}-\bar{r}}{l} = \frac{(x-u)\bar{e}_1 + [l_0 + (y-v)]\bar{e}_2}{l} \tag{A-5}$$

The spring elongation is

$$\Delta = l - l_0 \tag{A-6}$$

and if the spring stiffness is k, the spring restoring force is

$$\bar{F}_s = -k\Delta\bar{n} = -k\left(1-\frac{l_0}{l}\right)\{(x-u)\bar{e}_1 + [l_0+(y-v)]\bar{e}_2\} \tag{A-7}$$

The gravitational force is

$$\bar{F}_g = mg\bar{e}_2 \tag{A-8}$$

The equation of motion for the mass is

$$\bar{F}_s + \bar{F}_g = m\ddot{\bar{R}} \tag{A-9}$$

or

$$\ddot{x} = -\frac{k}{m}\left(1-\frac{l_0}{l}\right)(x-u) \tag{A-10}$$

$$\ddot{y} = g - \frac{k}{m}\left(1-\frac{l_0}{l}\right)[l_0+(y-v)] \tag{A-11}$$

The static solution is

$$u = v = 0 \tag{A-12}$$

$$\ddot{x} = \ddot{y} = 0 \tag{A-13}$$

$$x_{ST} = 0 \tag{A-14}$$

$$y_{ST} = l_{ST} - l_0 = \frac{mg}{k} \tag{A-15}$$

The static solution defines the initial conditions for a dynamic problem. To initiate a finite difference solution, we assume that $\ddot{x}$ and $\ddot{y}$ are constant during the first time interval.

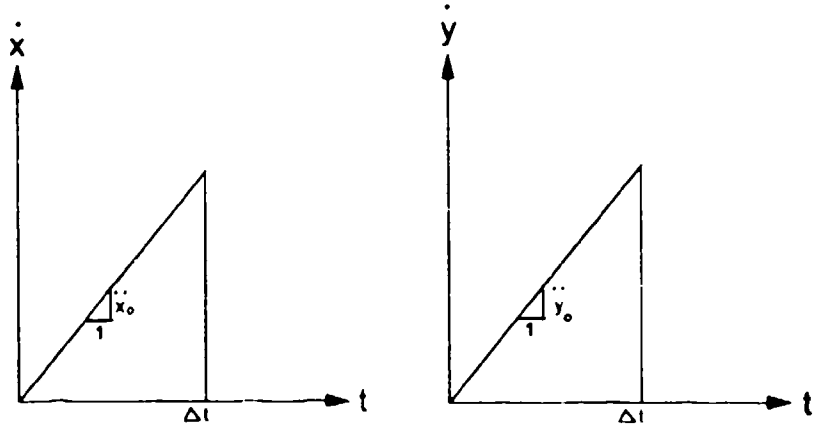

Therefore

$$x_1 = \frac{\ddot{x}_0(\Delta t)^2}{6} \tag{A-16}$$

$$y_1 = y_{ST} + \frac{\ddot{y}_0(\Delta t)^2}{6} \tag{A-17}$$

Equation (A-10) thus takes the form

$$\ddot{x}_0 = -\frac{k}{m}\left(1 - \frac{l_0}{l_{ST}}\right)\left[\frac{\ddot{x}_0(\Delta t)^2}{6} - u_1\right] \tag{A-18}$$

so that

$$\ddot{x}_0 = \frac{\frac{gu_1}{l_{ST}}}{1 + \frac{g(\Delta t)^2}{6l_{ST}}} = \frac{u_1}{\frac{l_{ST}}{g} + \frac{(\Delta t)^2}{6}} \tag{A-19}$$

and Equation (A-11) takes the form

$$\ddot{y}_0 = g - \frac{k}{m}\left[y_{ST} + \frac{\ddot{y}_0(\Delta t)^2}{6} - v_1\right] \tag{A-20}$$

so that

$$\ddot{y}_0 = \frac{\frac{kv_1}{m}}{1 + \frac{k(\Delta t)^2}{6m}} = \frac{v_1}{\frac{m}{k} + \frac{(\Delta t)^2}{6}} \tag{A-21}$$

From this point on, the finite difference solution proceeds smoothly.

Step 1: $x_0 = 0$

Step 2: $y_0 = \frac{mg}{k}$

Step 3: $x_1 = \left[\frac{\frac{g(\Delta t)^2}{6l_{ST}}}{1 + \frac{g(\Delta t)^2}{6l_{ST}}}\right] u_1$

Step 4: $$y_1 = \left[\frac{\frac{k(\Delta t)^2}{6m}}{1+\frac{k(\Delta t)^2}{6m}}\right] v_1 + y_o$$

For $n \geq 1$

Step 5: $$l_n = \sqrt{(x_n - u_n)^2 + [l_0 + (y_n - v_n)]^2}$$

Step 6: $$\beta_n = \frac{k}{m}\left(1 - \frac{l_0}{l_n}\right)$$

Step 7: $$\ddot{x}_n = -\beta_n (x_n - u_n)$$

Step 8: $$\ddot{y}_n = g - \beta_n [l_0 + (y_n - v_n)]$$

Step 9: $$x_{n+1} = 2x_n - x_{n-1} + \ddot{x}_n (\Delta t)^2$$

Step 10: $$y_{n+1} = 2y_n - y_{n-1} + \ddot{y}_n (\Delta t)^2$$

Return to step 5

This page is left blank

APPENDIX B

SPEND PROGRAM LISTING

```
      PROGRAM SPEND
C
C ***************************************************************
C *                                                             *
C *               ***   SPRING - PENDULUM   ***                 *
C *                                                             *
C *                                                             *
C *    Program calculates the response of a spring-pendulum     *
C *    subjected to a support motion in both the vertical       *
C *    and the horizontal direction.                            *
C *                                                             *
C *             Last Revision:  7 July 1992 (MAR)               *
C *                                                             *
C ***************************************************************
C
C  OPEN THE INPUT AND OUTPUT FILES
C
      IMPLICIT DOUBLE PRECISION (A-H,O-Z)
      CHARACTER INFILE*12
      PARAMETER (ID=8000)
      DIMENSION U(0:ID),V(0:ID),X(0:ID),Y(0:ID),XDD(0:ID),YDD(0:ID),
     &SF(0:ID)
C
      PRINT *,'    Input File Name ... '
      READ'(A12)',INFILE
      OPEN(UNIT=15,FILE=INFILE,STATUS='OLD')
      OPEN(UNIT=16,FILE='XDISP.',STATUS='UNKNOWN')
      OPEN(UNIT=17,FILE='YDISP.',STATUS='UNKNOWN')
      OPEN(UNIT=18,FILE='SFORCE.',STATUS='UNKNOWN')
      OPEN(UNIT=19,FILE='XACC.',STATUS='UNKNOWN')
      OPEN(UNIT=20,FILE='YACC.',STATUS='UNKNOWN')
C
C  READ THE INPUT DATA
C
C ***************************************************************
C *                                                             *
C *       DEFINITION OF INPUT VARIABLES:                        *
C *                                                             *
C *    PWT = PENDULUM WEIGHT (LBS)                              *
C *                                                             *
C *    STIFF = SPRING STIFFNESS (LBS/IN)                        *
C *                                                             *
C *    ULENGTH = UNDEFORMED LENGTH OF SPRING (IN)               *
C *                                                             *
C *    NPTS = # OF PTS. IN BASE DISPLACEMENT HISTORY            *
C *                                                             *
C *    DELT = TIME INCREMENT BETWEEN TIME POINTS (SEC)          *
C *                                                             *
C *    U(N) = HORIZONTAL BASE DISPLACEMENT @ TIME STEP "N"      *
C *              ( NOTE: U(0)=0.0 )                             *
C *                                                             *
C *    V(N) = VERTICAL BASE DISPLACEMENT @ TIME STEP "N"        *
C *              ( NOTE: V(0)=0.0 )                             *
C *                                                             *
C *                                                             *
C *       SIGN CONVENTION:                                      *
C *                                                             *
C *    DOWNWARD VERTICAL DISPLACEMENTS ARE POSITIVE             *
C *                                                             *
C *    SPRING TENSION IS POSITIVE                               *
```

```
C *                                                              *
C ****************************************************************
C
      READ(15,*) PWT,STIFF,ULENGTH,NPTS,DELT
      PRINT *,'   Reading Horizontal Base Motion'
      READ(15,*) (U(N), N=0,NPTS-1)
      PRINT *,'   Reading Vertical Base Motion'
      READ(15,*) (V(N), N=0,NPTS-1)
C
      PRINT *,'   Computing Pendulum Response'
C
C  ACCELERATION OF GRAVITY (IN/SEC**2)
C
      AGRAV=386.0
C
C  CALCULATE THE MASS OF THE PENDULUM (LB-SEC**2/IN)
C
      PMASS=PWT/AGRAV
C
C  CALCULATE PENDULUM DISPLACEMENTS @ TIME 0 (I.E., STATIC DEFLECTION)
C
      X(0)=0.0
      Y(0)=PWT/STIFF
      STATLEN=Y(0)+ULENGTH
C
C  CALCULATE DISPLACEMENT @ TIME STEP 1
C
      CON1=(AGRAV*DELT**2.)/(6.*STATLEN)
      X(1)=(CON1/(1+CON1))*U(1)
      CON2=(STIFF*DELT**2.)/(6.*PMASS)
      Y(1)=Y(0)+(CON2/(1+CON2))*V(1)
C
C  INITIALIZE ACCELERATIONS & SPRING FORCE @ TIME 0
C
      SF(0)=PWT
      XDD(0)=0.0
      YDD(0)=0.0
C
C  LOOP THRU TIME STEPS FROM N=1 TO NPTS-1
C
      DO 100 N=1,NPTS-1
C
      SPLEN=DSQRT((DABS(X(N)-U(N)))**2.+(ULENGTH+(Y(N)-V(N)))**2.)
C
C  ERROR TRAP:  FOR LOW FREQUENCY SYSTEMS, THE SPRING MAY BECOME
C               FULLY COMPRESSED.  THIS LEADS TO A DIVIDE BY ZERO
C               ERROR WHEN CALCULATING BETA.
C
      IF (SPLEN .LT. (0.1*ULENGTH)) THEN
      PRINT *,'   Excessive spring compression has occured!'
      STOP
      ENDIF
C
      BETA=(STIFF/PMASS)*(1-ULENGTH/SPLEN)
C
C  CALCULATE ACCELERATIONS @ TIME STEP N
C
      XDD(N)=-BETA*(X(N)-U(N))
      YDD(N)=AGRAV-BETA*(ULENGTH+(Y(N)-V(N)))
C
```

```
C  SPRING FORCE @ STEP N
C
      SF(N)=(SPLEN-ULENGTH)*STIFF
C
C  DISPLACEMENT @ STEP N+1
C
      X(N+1)=2.*X(N)-X(N-1)+XDD(N)*DELT**2.
      Y(N+1)=2.*Y(N)-Y(N-1)+YDD(N)*DELT**2.
C
 100  CONTINUE
C
C  WRITE OUTPUT FILES
C
      PRINT *,'   Saving Pendulum Response'
C
C  X-DISPLACEMENT
C
      WRITE(16,*) NPTS
      WRITE(16,*) DELT
      WRITE(16,*) (X(N), N=0,NPTS-1)
      CLOSE(16)
C
C  Y-DISPLACEMENT
C
      WRITE(17,*) NPTS
      WRITE(17,*) DELT
      WRITE(17,*) (Y(N), N=0,NPTS-1)
      CLOSE(17)
C
C  SPRING FORCE
C
      WRITE(18,*) NPTS
      WRITE(18,*) DELT
      WRITE(18,*) (SF(N), N=0,NPTS-1)
      CLOSE(18)
C
C  X-ACCELERATION
C
      WRITE(19,*) NPTS
      WRITE(19,*) DELT
      WRITE(19,*) (XDD(N), N=0,NPTS-1)
      CLOSE(19)
C
C  Y-ACCELERATION
C
      WRITE(20,*) NPTS
      WRITE(20,*) DELT
      WRITE(20,*) (YDD(N), N=0,NPTS-1)
      CLOSE(20)
C
      STOP
      END
```

APPENDIX C

TRANSIENT RESPONSE OF A CANTILEVER BEAM CARRYING A TIP MASS

Transient Response of a Cantilever Beam, Carrying a Tip Mass Having Both Translational and Rotary Inertia, to Support Motion

Consider the cantilever beam shown below, carrying a tip mass having both translational and rotary inertia.

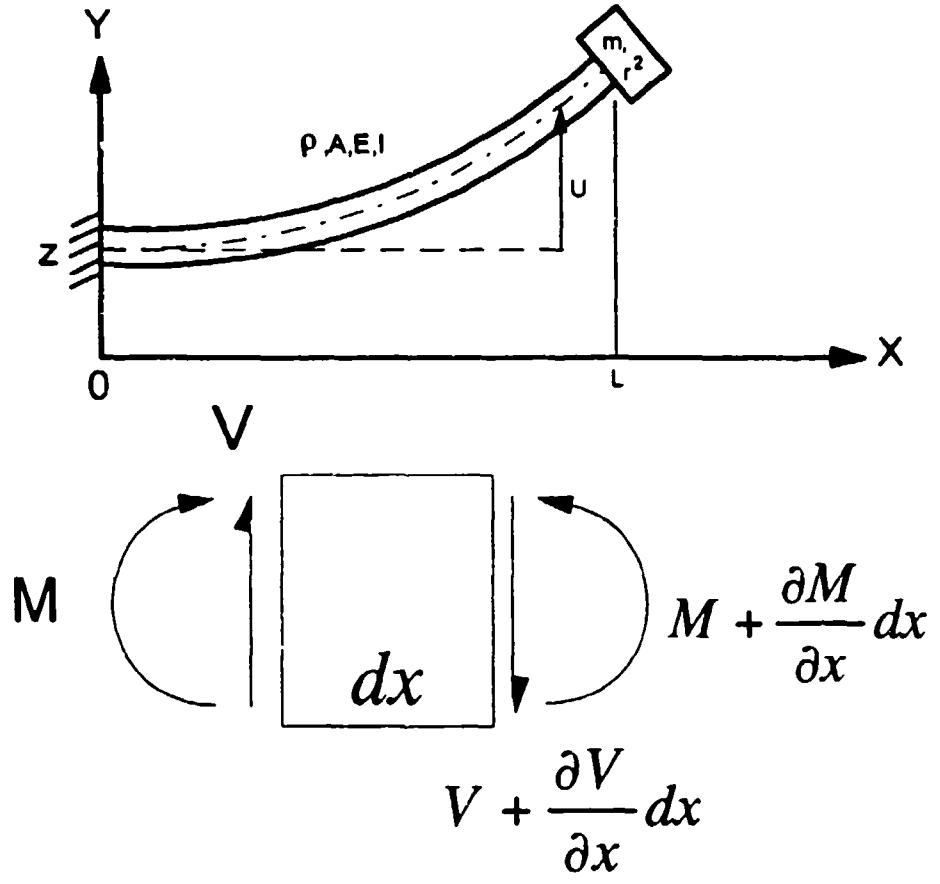

1. Governing Equation, Initial and Boundary Conditions

The total beam deflection is

$$y = z + u \tag{C-1}$$

where

z = support motion

u = beam deflection WRT the support

The equation of motion for a beam element is

$$-\frac{\partial V}{\partial x} dx = \rho A dx \frac{\partial^2 y}{\partial t^2} = \rho A dx \frac{\partial^2}{\partial t^2}(z + u) \tag{C-2}$$

Neglecting the beam element rotary inertia yields

$$V = \frac{\partial M}{\partial x} \tag{C-3}$$

and the beam moment-curvature relation is

$$M = EI\frac{\partial^2 u}{\partial x^2} \tag{C-4}$$

Substituting Equations (C-3) and (C-4) into Equation (C-2) yields

$$-EI\frac{\partial^4 u}{\partial x^4} = \rho A\frac{\partial^2 z}{\partial t^2} + \rho A\frac{\partial^2 u}{\partial t^2}$$

or

$$\frac{\partial^4 u}{\partial x^4} + \frac{\rho A}{EI}\frac{\partial^2 u}{\partial t^2} = -\frac{\rho A}{EI}\frac{\partial^2 z}{\partial t^2} \tag{C-5}$$

The initial and boundary conditions are:

$$y(x,0) = 0 \qquad (0 \le x \le L) \tag{C-6}$$

$$\frac{\partial y}{\partial t}(x,0) = 0 \qquad (0 \le x \le L) \tag{C-7}$$

$$u(0,t) = 0 \qquad (t \ge 0) \tag{C-8}$$

$$\frac{\partial u}{\partial x}(0,t) = 0 \qquad (t \ge 0) \tag{C-9}$$

$$EI\frac{\partial^2 u}{\partial x^2}(L,t) = -mr^2\frac{\partial^2}{\partial t^2}\left[\frac{\partial u}{\partial x}(L,t)\right] \qquad (t \ge 0) \tag{C-10}$$

$$EI\frac{\partial^3 u}{\partial x^3} = m\frac{\partial^2 y}{\partial t^2}(L,t) \qquad (t \ge 0) \tag{C-11}$$

Now let

$$\alpha = \frac{u}{L} \tag{C-12}$$

$$\beta = \frac{z}{L} \tag{C-13}$$

$$\xi = \frac{x}{L} \tag{C-14}$$

so that

$$\frac{\partial}{\partial x} = \frac{\partial}{\partial \xi}\frac{d\xi}{dx} = \frac{1}{L}\frac{d}{d\xi} \tag{C-15}$$

Then Equation (C-5) can be written in the form

$$\frac{\partial^4\alpha}{\partial\xi^4}+\frac{\rho AL^4}{EI}\frac{\partial^2\alpha}{\partial t^2}=\frac{\rho AL^4}{EI}\frac{\partial^2\beta}{\partial t^2} \tag{C-16}$$

and if we set

$$T=L^2\sqrt{\frac{\rho A}{EI}} \tag{C-17}$$

and

$$\psi=\frac{t}{T} \tag{C-18}$$

so that

$$\frac{\partial}{\partial t}=\frac{\partial}{\partial\psi}\frac{d\psi}{dt}=\frac{1}{T}\frac{\partial}{\partial\psi} \tag{C-19}$$

then Equation (C-16) can be written in the final dimensionless form

$$\frac{\partial^4\alpha}{\partial\xi^4}+\frac{\partial^2\alpha}{\partial\psi^2}=\frac{\partial^2\beta}{\partial\psi^2} \tag{C-20}$$

with the initial and boundary conditions

$$\alpha(\xi,0)=0 \qquad (0\le\xi\le1) \tag{C-21}$$

$$\frac{\partial\alpha}{\partial\psi}(\xi,0)=-\frac{\partial\beta}{\partial\psi}(0) \qquad (0\le\xi\le1) \tag{C-22}$$

$$\alpha(0,\psi)=0 \qquad (\psi\ge0) \tag{C-23}$$

$$\frac{\partial\alpha}{\partial\xi}(0,\psi)=0 \qquad (\psi\ge0) \tag{C-24}$$

$$\frac{\partial^2\alpha}{\partial\xi^2}(1,\psi)=-\frac{mr^2}{\rho AL^3}\left[\frac{\partial^3\alpha}{\partial\xi\partial\psi^2}(1,\psi)\right] \qquad (\psi\ge0) \tag{C-25}$$

$$\frac{\partial^3\alpha}{\partial\xi^3}(1,\psi)=\frac{m}{\rho AL}\left[\frac{\partial^2\alpha}{\partial\psi^2}(1,\psi)+\frac{\partial^2\beta}{\partial\psi^2}(\psi)\right] \qquad (\psi\ge0) \tag{C-26}$$

We first consider the homogeneous form of Equation (C-20),

$$\frac{\partial^4\alpha}{\partial\xi^4}+\frac{\partial^2\alpha}{\partial\psi^2}=0 \tag{C-27}$$

because it turns out to generate a family of orthogonal functions (free vibration modes) that can be used to solve the nonhomogeneous problem.

We assume that

$$\alpha(\xi,\psi) = \phi(\xi)\dot{\theta}(\psi) \tag{C-28}$$

so that, setting

$$\frac{d\phi}{d\xi} = \phi' \tag{C-29}$$

$$\frac{d\theta}{d\psi} = \dot{\theta} \tag{C-30}$$

substituting Equation (C-28) into Equation (C-27) yields

$$\phi^{IV}\theta + \phi\ddot{\theta} = 0 \tag{C-31}$$

or, dividing by $\phi\theta$,

$$\frac{\phi^{IV}}{\phi} + \frac{\ddot{\theta}}{\theta} = 0 \tag{C-32}$$

Equation (C-32) says the sum of two independent quantities (one a function of space, the other a function of time) is zero; therefore they must both be constant. We therefore set

$$\frac{\phi^{IV}}{\phi} = -\frac{\ddot{\theta}}{\theta} = \lambda^4 \tag{C-33}$$

so that ϕ and θ must obey the equations

$$\phi^{IV} - \lambda^4\phi = 0 \tag{C-34}$$

$$\ddot{\theta} + \lambda^4\theta = 0 \tag{C-35}$$

The solution to Equation (C-34) can be written in the form

$$\phi = Af_1 + Bf_2 + Cf_3 + Df_4 \tag{C-36}$$

where

$$f_1 = \cosh\lambda\xi + \cos\lambda\xi \tag{C-37}$$

$$f_2 = \sinh\lambda\xi - \sin\lambda\xi \tag{C-38}$$

$$f_3 = \cosh\lambda\xi - \cos\lambda\xi \tag{C-39}$$

$$f_4 = \sinh\lambda\xi + \sin\lambda\xi \tag{C-40}$$

so that

$$\phi' = \lambda(Af_2 + Bf_3 + Cf_4 + Df_1) \tag{C-41}$$

$$\phi'' = \lambda^2(Af_3 + Bf_4 + Cf_1 + Df_2) \tag{C-42}$$

$$\phi''' = \lambda^3(Af_4 + Bf_1 + Cf_2 + Df_3) \tag{C-43}$$

$$\phi^{IV} = \lambda^4 (Af_1 + Bf_2 + Cf_3 + Df_4) = \lambda^4 \phi \tag{C-44}$$

Now

$$f_1(0) = 2 \tag{C-45}$$

$$f_2(0) = f_3(0) = f_4(0) = 0 \tag{C-46}$$

so that Equations (C-23) and (C-36) yield

$$\phi(0) = 2A = 0 \tag{C-47}$$

and Equations (C-24) and (C-41) yield

$$\phi'(0) = 2\lambda D = 0 \tag{C-48}$$

so that

$$A = D = 0 \tag{C-49}$$

If we now set

$$f_i(1) = F_i \tag{C-50}$$

$$\frac{n'}{\rho AL} = k_1 \tag{C-51}$$

$$\left(\frac{r}{L}\right)^2 = k_2 \tag{C-52}$$

then Equations (C-25), (C-41), and (C-42) yield

$$\phi''(1)\theta = -k_1 k_2 \phi'(1)\ddot{\theta} \tag{C-53}$$

or

$$\lambda^2 (BF_4 + CF_1) = k_1 k_2 \lambda^5 (BF_3 + CF_4)$$

or

$$B(F_4 - k_1 k_2 \lambda^3 F_3) + C(F_1 - k_1 k_2 \lambda^3 F_4) = 0 \tag{C-54}$$

and Equations (C-26), (C-36), and (C-43) yield

$$\phi'''(1)\theta = k_1 \phi(1)\ddot{\theta} \tag{C-55}$$

or

$$\lambda^3 (BF_1 + CF_2) = -k_1 \lambda^4 (BF_2 + CF_3)$$

or

$$B(F_1 + k_1 \lambda F_2) + C(F_2 + k_1 \lambda F_3) = 0 \tag{C-56}$$

Equations (C-54) and (C-56) yield the relative values of B and C.

$$\frac{C}{B} = -\frac{F_4 - k_1 k_2 \lambda^3 F_3}{F_1 - k_1 k_2 \lambda^3 F_4} = -\frac{F_1 + k_1 \lambda F_2}{F_2 + k_1 \lambda F_3} = \rho \tag{C-57}$$

so that

$$(F_2 + k_1 \lambda F_3)(F_4 - k_1 k_2 \lambda^3 F_3) - (F_1 + k_1 \lambda F_2)(F_1 - k_1 k_2 \lambda^3 F_4) = 0 \tag{C-58}$$

For each root of Equation (C-58), λ_i, there is a ratio

$$\frac{C_i}{B_i} = \rho_i \tag{C-59}$$

given by Equation (C-57).

2. Orthogonality of Vibration Mode Shapes

Now consider the incremental work done by the end actions associated with mode i, acting through incremental displacements associated with mode j.

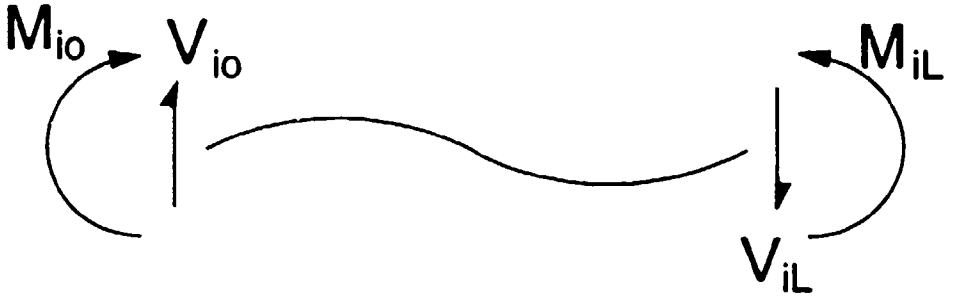

$$\delta W_{ij} = V_{i0}\delta y_{j0} - M_{i0}\delta\frac{\partial u_{j0}}{\partial x} - V_{iL}\delta y_{jL} + M_{iL}\delta\frac{\partial u_{jL}}{\partial x} \tag{C-60}$$

Now

$$M = EI\frac{\partial^2 u}{\partial x^2} = \frac{EI}{L}\phi''\theta \tag{C-61}$$

$$V = EI\frac{\partial^3 u}{\partial x^3} = \frac{EI}{L^2}\phi'''\theta \tag{C-62}$$

$$u = L\phi\theta \tag{C-63}$$

$$\frac{\partial u}{\partial x} = \phi'\theta \tag{C-64}$$

so that Equation (C-60) can be written in the form

$$\delta W_{ij} = \frac{EI}{L}\theta_i\delta\theta_j\left[\phi_i''\phi_j' - \phi_i'''\phi_j\right]_0^1 \tag{C-65}$$

$$= \frac{EI}{L}\theta_i\delta\theta_j\int_0^1\left(\phi_i'''\phi_j' + \phi_i''\phi_j'' - \phi_i^{IV}\phi_j - \phi_i'''\phi_j'\right)d\xi$$

$$= \frac{EI}{L}\theta_i\delta\theta_j\int_0^1\left(\phi_i''\phi_j'' - \lambda_i^4\phi_i\phi_j\right)d\xi \tag{C-66}$$

Eliminating δW_{ij} between Equations (C-65) and (C-66) yields

$$\int_0^1 \phi_i'' \phi_j'' d\xi = \lambda_i^4 \int_0^1 \phi_i \phi_j d\xi + \left[\phi_i'' \phi_j' - \phi_i''' \phi_j \right]_0^1 \tag{C-67}$$

Since the LHS of Equation (C-67) is symmetric with respect to i and j, the RHS must be also, so that

$$\int_0^1 \phi_i'' \phi_j'' d\xi = \lambda_j^4 \int_0^1 \phi_i \phi_j d\xi + \left[\phi_i' \phi_j'' - \phi_i \phi_j''' \right]_0^1 \tag{C-68}$$

Eliminating $\int_0^1 \phi_i'' \phi_j'' d\xi$ between Equations (C-67) and (C-68) yields

$$\left(\lambda_j^4 - \lambda_i^4 \right) \int_0^1 \phi_i \phi_j d\xi + \left[\phi_j \phi_i''' - \phi_j' \phi_i'' + \phi_j'' \phi_i' - \phi_j''' \phi_i \right]_0^1 = 0 \tag{C-69}$$

Now

$$\phi(0) = 0 \tag{C-70}$$

$$\phi'(0) = 0 \tag{C-71}$$

and if we set

$$\phi(1) = \Phi \tag{C-72}$$

then Equations (C-33) and (C-53) yield

$$\Phi'' = k_1 k_2 \lambda^4 \Phi' \tag{C-73}$$

and Equations (C-33) and (C-55) yield

$$\Phi''' = -k_1 \lambda^4 \Phi \tag{C-74}$$

so that Equation (C-69) yields

$$\left(\lambda_j^4 - \lambda_i^4 \right) \int_0^1 \phi_i \phi_j d\xi + \left[-k_1 \lambda_i^4 \Phi_i \Phi_j - k_1 k_2 \lambda_i^4 \Phi_i' \Phi_j' + k_1 k_2 \lambda_j^4 \Phi_i' \Phi_j' + k_1 \lambda_j^4 \Phi_i \Phi_j \right]$$

$$= \left(\lambda_j^4 - \lambda_i^4 \right) \left(\int_0^1 \phi_i \phi_j d\xi + k_1 \Phi_i \Phi_j + k_1 k_2 \Phi_i' \Phi_j' \right) = 0 \tag{C-75}$$

When $j \neq i$ the second factor on the LHS of Equation (C-75) must be zero, and when $j = i$ that factor is arbitrary. Thus we can set

$$\int_0^1 \phi_i \phi_j d\xi + k_1 \Phi_i \Phi_j + k_1 k_2 \Phi_i' \Phi_j' = \delta_{ij} \tag{C-76}$$

Equation (C-76) would be most useful if the integral were expressed in terms of boundary values. This can be done by returning to Equation (C-69), and writing it in the form [cf Prescott (1924:223), Eq. (9.111)]

$$\int_0^1 \phi_i \phi_j d\xi = \frac{\left[\phi_j''' \phi_i - \phi_j'' \phi_i' + \phi_j' \phi_i'' - \phi_j \phi_i''' \right]_0^1}{\lambda_j^4 - \lambda_i^4} \tag{C-77}$$

Treating λ_i as a constant and λ_j as a variable, applying L'Hospital's rule to the case in which $\lambda_j = \lambda_i$, and noting that

$$\frac{d}{d\lambda}[\phi(\lambda\xi)] = \frac{d\phi}{d(\lambda\xi)}\frac{d(\lambda\xi)}{d\lambda} = \xi\frac{d\phi}{d(\lambda\xi)} \tag{C-78}$$

$$\phi' = \frac{d}{d\xi}[\phi(\lambda\xi)] = \frac{d\phi}{d(\lambda\xi)}\frac{d(\lambda\xi)}{d\xi} = \lambda\frac{d\phi}{d(\lambda\xi)} \tag{C-79}$$

so that

$$\frac{d\phi}{d\lambda} = \frac{\xi}{\lambda}\phi' \tag{C-80}$$

Equation (C-77) yields

$$\int_0^1 \phi_i^2 d\xi = \frac{\left\{\xi\left[\phi_i^{IV}\phi_i - \phi_i'''\phi_i' + (\phi_i'')^2 - \phi_i'\phi_i'''\right]\right\}_0^1}{4\lambda_i^4}$$

$$= \frac{\lambda_i^4\Phi_i^2 + 2k_1\lambda_i^4\Phi_i\Phi_i' + k_1^2k_2^2\lambda_i^8(\Phi_i')^2}{4\lambda_i^4}$$

$$= \frac{\Phi_i^2 + 2k_1\Phi_i\Phi_i' + k_1^2k_2^2\lambda_i^4(\Phi_i')^2}{4} \tag{C-81}$$

Therefore, when $i = j$, Equation (C-76) can be written in the form

$$\frac{\Phi_i^2 + 2k_1\Phi_i\Phi_i' + k_1^2k_2^2\lambda_i^4(\Phi_i')^2}{4} + k_1\Phi_i^2 + k_1k_2(\Phi_i')^2 = 1$$

or

$$(1+4k_1)\Phi_i^2 + 2k_1\Phi_i\Phi_i' + k_1k_2\left(4 + k_1k_2\lambda_i^4\right)(\Phi_i')^2 = 4 \tag{C-82}$$

Now Equations (C-36), (C-37), and (C-50) yield

$$\Phi = BF_2 + CF_3 \tag{C-83}$$

$$\Phi' = \lambda(BF_3 + CF_4) \tag{C-84}$$

and therefore

$$\Phi^2 = F_2^2B^2 + 2F_2F_3BC + F_3^2C^2 \tag{C-85}$$

$$\Phi\Phi' = \lambda\left[F_2F_3B^2 + \left(F_2F_4 + F_3^2\right)BC + F_3F_4C^2\right] \tag{C-86}$$

$$(\Phi')^2 = \lambda^2\left(F_3^2B^2 + 2F_3F_4BC + F_4^2C^2\right) \tag{C-87}$$

and thus Equation (C-82) can be written in the form

$$\Lambda_1B^2 + \Lambda_2BC + \Lambda_3C^2 = 4 \tag{C-88}$$

where

$$\Lambda_1 = (1+4k_1)F_2^2 + 2k_1\lambda_i F_2 F_3 + k_1 k_2\left(4 + k_1 k_2 \lambda_i^4\right)\lambda_i^2 F_3^2 \tag{C-89}$$

$$\Lambda_2 = 2\left[(1+4k_1)F_2 F_3 + k_1\lambda_i\left(F_2 F_4 + F_3^2\right) + k_1 k_2\left(4 + k_1 k_2 \lambda_i^4\right)\lambda_i^2 F_3 F_4\right] \tag{C-90}$$

$$\Lambda_3 = (1+4k_1)F_3^2 + 2k_1\lambda_i F_3 F_4 + k_1 k_2\left(4 + k_1 k_2 \lambda_i^4\right)\lambda_i^2 F_4^2 \tag{C-91}$$

Substituting Equation (C-59) into Equation (C-88) then yields

$$B_i^2\left(\Lambda_1 + \Lambda_2\rho_i + \Lambda_3\rho_i^2\right) = 4 \tag{C-92}$$

so that

$$B_i = \frac{2}{\sqrt{\Lambda_1 + \Lambda_2\rho_i + \Lambda_3\rho_i^2}} \tag{C-93}$$

and

$$C_i = \rho_i B_i \tag{C-94}$$

Finally, combining Equations (C-67), (C-73), (C-74), and (C-76) yields

$$\int_0^1 \left(\phi_i''\right)^2 d\xi = \lambda_i^4 \tag{C-95}$$

3. Derivation of Modal Equation of Motion by Hamilton's Principle

Let

$$u(x,t) = \sum_{i=1}^{\bar{n}} \eta_i(x) q_i(t)$$

and

$$z(t) = u_g(t)$$

then

$$y(x,t) = u(x,t) + z(t)$$

$$= \sum_{i=1}^{\bar{n}} \eta_i(x) q_i(t) + u_g(t) \tag{C-96}$$

The kinetic energy of the system is

$$T = \frac{1}{2}\int_0^L \rho A\left(\frac{\partial y}{\partial t}\right)^2 dx + \frac{1}{2} m\left(\frac{\partial y}{\partial t}\right)_L^2 + \frac{1}{2} m r^2\left(\frac{\partial^2 y}{\partial t \partial x}\right)_L^2 \tag{C-97}$$

and the strain energy of the system is

$$U = \frac{1}{2}\int_0^L EI\left(\frac{\partial^2 u}{\partial x^2}\right)^2 dx \tag{C-98}$$

Applying Hamilton's Principle to obtain the equation of motion:

$$\int_{t_1}^{t_2} \delta(T-U)dt = 0 \tag{C-99}$$

$$\delta T = \int_0^L \rho A \dot{y}\delta\dot{y}dx + m\dot{y}_L\delta\dot{y}_L + mr^2\dot{u}_L'\delta\dot{u}_L' \tag{C-100}$$

$$\delta U = \int_0^L EIu''\delta u''dx \tag{C-101}$$

where

$$\dot{y} = \sum_{i=1}^{\infty}\eta_i\dot{q}_i + \dot{u}_g \tag{C-102}$$

$$\delta\dot{y} = \delta\dot{u} = \sum_{i=1}^{\infty}\eta_i\delta\dot{q}_i \tag{C-103}$$

$$\dot{y}_L = \dot{u}_L + \dot{u}_g = \sum_{i=1}^{\infty}\eta_i(L)\dot{q}_i + \dot{u}_g \tag{C-104}$$

$$\delta\dot{y}_L = \delta\dot{u}_L = \sum_{i=1}^{\infty}\eta_i(L)\delta\dot{q}_i \tag{C-105}$$

$$u' = \sum_{i=1}^{\infty}\eta_i'q_i \tag{C-106}$$

$$u' = \sum_{i=1}^{\infty}\eta_i'\dot{q}_i \tag{C-107}$$

$$\dot{u}_L' = \sum_{i=1}^{\infty}\eta_i'(L)\dot{q}_i \tag{C-108}$$

$$\delta\dot{u}_L' = \sum_{i=1}^{\infty}\eta_i'(L)\delta\dot{q}_i \tag{C-109}$$

$$u'' = \sum_{i=1}^{\infty}\eta_i''q_i \tag{C-110}$$

$$\delta u'' = \sum_{i=1}^{\infty}\eta_i''\delta q_i \tag{C-111}$$

Equation (C-99) can be expressed as

$$\int_{t_1}^{t_2}\left[\int_0^L \rho A\left(\sum\eta\dot{q} + \dot{u}_g\right)\left(\sum\eta_i\delta\dot{q}\right)dx + m\left(\sum\eta(L)\dot{q} + \dot{u}_g\right)\left(\sum\eta(L)\delta\dot{q}\right)\right.$$

$$+mr^2\left(\sum \eta'(L)\dot{q}\right)\left(\sum \eta'(L)\delta\dot{q}\right)-\int_0^L EI\left(\sum \eta'' q\right)\left(\sum \eta''\delta q\right)dx\Big]dt=0 \qquad \text{(C-112)}$$

$$\int_0^L \rho A\left(\sum \eta\dot{q}+\dot{u}_g\right)\left(\sum \eta\delta\dot{q}\right)dx=\sum_{i=1}^{\bar{n}}\sum_{j=1}^{\bar{n}}\dot{q}_i\delta\dot{q}_j\int_0^L\rho A\,\eta_i\eta_j dx+\dot{u}_g\sum_{i=1}^{\bar{n}}\delta\dot{q}_i\int_0^L\rho A\,\eta_i dx \qquad \text{(C-113)}$$

$$m\left(\sum \eta(L)\dot{q}+\dot{u}_g\right)\left(\sum \eta(L)\delta\dot{q}\right)=m\sum_{i=1}^{\bar{n}}\sum_{j=1}^{\bar{n}}\dot{q}_i\delta\dot{q}_j\eta_i(L)\eta_j(L)+m\dot{u}_g\sum_{i=1}^{\bar{n}}\delta\dot{q}_i\eta_i(L) \qquad \text{(C-114)}$$

$$mr^2\left(\sum \eta'(L)\dot{q}\right)\left(\sum \eta'(L)\delta\dot{q}\right)=mr^2\sum_{i=1}^{\bar{n}}\sum_{j=1}^{\bar{n}}\dot{q}_i\delta\dot{q}_j\eta_i'(L)\eta_j'(L) \qquad \text{(C-115)}$$

$$\int_0^L EI\left(\sum \eta'' q\right)\left(\sum \eta''\delta q\right)dx=\sum_{i=1}^{\bar{n}}\sum_{j=1}^{\bar{n}}q_i\delta q_j\int_0^L EI\eta_i''\eta_j''dx \qquad \text{(C-116)}$$

Integrating Equation (C-112) by parts and using Equations (C-113) through (C-116),

$$\sum_{i=1}^{\bar{n}}\sum_{j=1}^{\bar{n}}\left(\int_0^L\rho A\,\eta_i\eta_j dx\,\dot{q}_i\delta q_j\Big|_{t_1}^{t_2}-\int_{t_1}^{t_2}\ddot{q}_i\delta q_j\int_0^L\rho A\,\eta_i\eta_j dx dt\right)$$

$$+\sum_{i=1}^{\bar{n}}\left(\dot{u}_g\int_0^L\rho A\,\eta_i dx\,\delta q_i\Big|_{t_1}^{t_2}-\int_{t_1}^{t_2}\ddot{u}_g\delta q_i\int_0^L\rho A\,\eta_i dx dt\right)$$

$$+m\sum_{i=1}^{\bar{n}}\sum_{j=1}^{\bar{n}}\left(\eta_i(L)\eta_j(L)\dot{q}_i\delta q_j\Big|_{t_1}^{t_2}-\int_{t_1}^{t_2}\ddot{q}_i\delta q_j\eta_i(L)\eta_j(L)dt\right)$$

$$+m\sum_{i=1}^{\bar{n}}\left(\dot{u}_g\eta_i(L)\delta q_i\Big|_{t_1}^{t_2}-\int_{t_1}^{t_2}\ddot{u}_g\delta q_i\eta_i(L)dt\right)$$

$$+mr^2\sum_{i=1}^{\bar{n}}\sum_{j=1}^{\bar{n}}\left(\eta_i'(L)\eta_j'(L)\dot{q}_i\delta q_j\Big|_{t_1}^{t_2}-\int_{t_1}^{t_2}\ddot{q}_i\delta q_j\eta_i'(L)\eta_j'(L)dt\right)$$

$$-\sum_{i=1}^{\bar{n}}\sum_{j=1}^{\bar{n}}q_i\delta q_j\int_0^L EI\eta_i''\eta_j''dxdt=0 \qquad \text{(C-117)}$$

Rearranging terms yields

$$\sum_{i=1}^{\bar{n}}\sum_{j=1}^{\bar{n}}\int_{t_1}^{t_2}\left\{\ddot{q}_i\left[\int_0^L\rho A\,\eta_i\eta_j dx+m\eta_i(L)\eta_j(L)+mr^2\eta_i'(L)\eta_j'(L)\right]+q_i\int_0^L EI\eta_i''\eta_j''dx\right\}\delta q_j dt$$

$$= -\sum_{i=1}^{\infty} \int_{t_1}^{t_2} \ddot{u}_g \left[\int_0^L \rho A \, \eta_i dx + m \eta_i(L) \right] \delta q_i dt \tag{C-118}$$

The orthogonality relations have been shown as

$$\int_0^L \rho A \, \eta_i \eta_j dx + m \eta_i(L) \eta_j(L) + m r^2 \eta_i'(L) \eta_j'(L) = \bar{\delta}_{ij} \tag{C-119}$$

and

$$\left.\begin{aligned} \int_0^L EI \eta_i'' \eta_j'' dx = 0 \qquad & \text{for} \qquad i \neq j \\ = \frac{EI}{L^3} \lambda_i^4 \qquad & \text{for} \qquad i = j \end{aligned}\right\} \tag{C-120}$$

Substituting Equations (C-119) and (C-120) into Equation (C-118),

$$\int_{t_1}^{t_2} \sum_{i=1}^{\infty} \left(\ddot{q}_i + \frac{EI}{L^3} \lambda_i^4 q_i + \ddot{u}_g \left[\int_0^L \rho A \eta_i dx + m \eta_i(L) \right] \right) \delta q_i dt = 0 \tag{C-121}$$

Since δq_i are arbitrary variations, it is necessary that

$$\ddot{q}_i + \frac{EI}{L^3} \lambda_i^4 q_i = -\ddot{u}_g \left[\int_0^L \rho A \, \eta_i dx + m \eta_i(L) \right] \tag{C-122}$$

for all i's. Equation (C-122) is the equation of motion for mode i. The nondimensional form of Equation (C-122) can be expressed as

$$\ddot{\theta}_i + \frac{\lambda_i^4}{T} \theta_i = -\ddot{\beta} \left[\int_0^1 \phi_i d\xi + k_i \phi_i(1) \right] \tag{C-123}$$